Resolving Knudsen Layer by High Order Moment Expansion

Yuwei Fan[*] Jun Li[†] Ruo Li[‡] Zhonghua Qiao[§]

April 19, 2022

Abstract

We model the Knudsen layer in Kramers' problem by the linearized high order hyperbolic moment system. Thanks to the hyperbolicity of the moment system, its boundary conditions are properly reduced from the kinetic boundary condition. For the Kramers' problem, we present the analytical solutions of the linearized moment systems. The velocity profile in the Knudsen layer is captured with improved accuracy for a wide range of accommodation coefficients. With the order of the moment system increasing, the velocity profile approaches to that of the linearized Boltzmann-BGK equation.

1 Introduction

In the area of gas kinetic theory, Kramers' problem [23] is generally considered as the most basic way to understand the effect of a wall on the flow behavior. The problem defines the Knudsen layer [26] without some of the additional complications in other more realistic problems, such as flow in a plane channel [14] or cylindrical tube [20, 16]. It is well-known [21, 43] that the classical Navier-Stokes-Fourier(NSF) equations with appropriate boundary conditions can be used to describe the flow with satisfactory accuracy when the gas is close to a statistical equilibrium state. However, a more accurate model is demanded to depict the nonequilibrium effects near the wall, where the continuum assumption is fundamentally broken down, and NSF equations themselves become inappropriate [26, 12]. This is exactly the case in Knudsen layers.

During the past decades, various methods [23, 30, 29, 37, 42, 27] have been developed to investigate the Kramers' problem based on the Boltzmann equation. Highly accurate results on the dependence of slip coefficient for the Boltzmann equation and general boundary condition have been reported [28, 30, 22]. Variable collision frequency models of the Boltzmann equation [10, 42, 28, 31, 29, 37] are extensively discussed. We note that the direct simulation Monte Carlo (DSMC) method [2] is widely used to solve the Boltzmann equation numerically. Unfortunately, DSMC calculations impose prohibitive computational demands for many applications of current interests. The intensive computational demands of DSMC method have motivated recent interests in the application of higher-order hydrodynamic models to simulate rarefied flows [36, 19, 18, 34]. There are many competing sets of higher-order constitutive relations, which are derived from the fundamental Boltzmann equation using different approaches. The classical approaches are the Grad's moment method[15] and the Chapman-Enskog technique[11]. Among these alternative macroscopic modeling and simulation strategies [15, 25], the moment method is quite attractive due to its numerous advantages [35, 39, 40]. It is regarded as a useful tool to extend classical fluid dynamics and achieves highly accurate approximations with high efficiency.

The moment method for gas kinetic theory [15] has been applied on wall-bounded geometries which are supplemented by slip and jump boundary conditions [32], while its application is seriously limited due to the lack of hyperbolicity [35, 6]. Particularly for the 3D case, the moment system is not hyperbolic in any neighborhood of the thermodynamic equilibrium. Only recently this fatal defect has been remedied [4, 5, 13]

[*]Department of Mathematics, Stanford University, Stanford, CA 94305, email: ywfan@stanford.edu.

[†]School of Mathematical Sciences, Peking University, Beijing, China, email: lijun609@pku.edu.cn.

[‡]CAPT, LMAM & School of Mathematical Sciences, Peking University, Beijing, China, email: rli@math.pku.edu.cn.

[§]Department of Applied Mathematics, the Hong Kong Polytechnic University, Hung Hom, Hong Kong, email:zhonghua.qiao@polyu.edu.hk.

that globally hyperbolic models can be deduced. The global hyperbolicity of the new models provides us the information propagation directions, and thus a proper boundary condition of the moment model may be proposed. This motivates us to study the Kramers' problem using the new moment models.

Starting from the globally Hyperbolic Moment Equations(HME), we first derive a linearized version of the HME to depict the Kramers' problem. We find that the linearized HME is even simpler than one's expectation since the equations related to the velocity are decoupled from other equations in the system involving high order moments. The number of equations in the decoupled part related to the velocity is the same as the moment expansion order only. Then we establish the boundary conditions for the linearized moment model according to physical and mathematical requirements for the system. Following Grad's approach in [15] for Maxwell's accommodation boundary condition [33], we propose a boundary condition for the HME. After that, by linearizing the macroscopic velocity and high order expansion coefficients for the boundary conditions, we present the boundary condition for the linearized HME. This prompts us to solve the decoupled system related to the velocity together with the corresponding boundary condition to obtain the velocity profile. It is proved that the analytical solution of the linearized HME with its boundary condition is unique for almost all accommodation coefficients in Maxwell's boundary condition. This indicates the boundary condition for the HME is well-posed in the sense of linearization, which provides the theoretical basis for the well-posedness of the boundary condition of the HME [7, 9].

Based on the analytical results of linearized HME, we study the slip coefficient, velocity defect and effective viscosity of the linearized HME quantitatively, and compare them with those of the linearized Boltzmann-BGK equation [37] and some existing models in [31, 17]. With not too many moments, the linearized HME can capture the Knudsen layer very well with a wide range of accommodation coefficients. Meanwhile, the analytical expressions of linearized HME can be used to provide a convenient correction near the wall [27] for the lower order macroscopic system, such as NSF equations. Moreover, we show that the velocity profile of the linearized HME has a good agreement with that of the linearized Boltzmann-BGK equation as the moment order increasing.

This paper is organized as follows. In Section 2 we review the HME for Boltzmann equations and derive the linearized HME. The boundary conditions for HME and its linearization are established in Section 3. The solutions of the linearized HME are solved in detail for Kramers' problem in Section 4. Properties of the velocity profile are well studied in Section 5. The paper ends with a conclusion and discussion.

2 The Linearized HME for the Boltzmann Equation

2.1 The Boltzmann equation

In gas kinetic theory, the motion of particles of a gas can be depicted by the Boltzmann equation [3]

$$\frac{\partial f}{\partial t} + \boldsymbol{\xi} \cdot \nabla_{\boldsymbol{x}} f = Q(f), \tag{2.1}$$

where $f(t, \boldsymbol{x}, \boldsymbol{\xi})$ is the number density distribution function which depends on the time $t \in \mathbb{R}^+$, the spatial position $\boldsymbol{x} \in \mathbb{R}^3$ and the microscopic particle velocity $\boldsymbol{\xi} \in \mathbb{R}^3$, and $Q(f)$ is the collision term. In this paper, we limit the discussion on the BGK collision model [1], which reads:

$$Q(f) = \frac{\rho\theta}{\mu}(\mathcal{M} - f), \tag{2.2}$$

where μ is the viscosity and $\mathcal{M}$ is the local thermodynamic equilibrium

$$\mathcal{M} = \frac{\rho}{(2\pi\theta)^{3/2}} \exp\left(-\frac{|\boldsymbol{\xi} - \boldsymbol{u}|^2}{2\theta}\right).$$

Here the density ρ, the macroscopic velocity $\boldsymbol{u}$ and the temperature θ are related to the distribution function f as

$$\rho = \int_{\mathbb{R}^3} f \,\mathrm{d}\boldsymbol{\xi}, \qquad \rho\boldsymbol{u} = \int_{\mathbb{R}^3} \boldsymbol{\xi} f \,\mathrm{d}\boldsymbol{\xi}, \qquad \rho|\boldsymbol{u}|^2 + 3\rho\theta = \int_{\mathbb{R}^3} |\boldsymbol{\xi}|^2 f \,\mathrm{d}\boldsymbol{\xi}. \tag{2.3}$$

Multiplying the Boltzmann equation by $(1, \boldsymbol{\xi}, |\boldsymbol{\xi}|^2)$ and integrating both sides over $\mathbb{R}^3$ with respect to $\boldsymbol{\xi}$, we obtain the conservation laws of mass, momentum, and energy as

$$\begin{aligned} &\frac{\mathrm{D}\rho}{\mathrm{D}t} + \rho \sum_{d=1}^{3} \frac{\partial u_d}{\partial x_d} = 0, \\ &\rho \frac{\mathrm{D}u_i}{\mathrm{D}t} + \sum_{d=1}^{3} \frac{\partial p_{id}}{\partial x_d} = 0, \quad i = 1, 2, 3, \\ &\frac{3}{2}\rho \frac{\mathrm{D}\theta}{\mathrm{D}t} + \sum_{k,d=1}^{3} p_{kd} \frac{\partial u_k}{\partial x_d} + \sum_{d=1}^{3} \frac{\partial q_d}{\partial x_d} = 0, \end{aligned} \tag{2.4}$$

where $\dfrac{\mathrm{D}\cdot}{\mathrm{D}t} := \dfrac{\partial \cdot}{\partial t} + \sum_{d=1}^{3} u_d \dfrac{\partial \cdot}{\partial x_d}$ is the material derivative, and the pressure tensor p_{ij} and the heat flux q_i are defined by

$$p_{ij} = \int_{\mathbb{R}^3} (\xi_i - u_i)(\xi_j - u_j) f \,\mathrm{d}\boldsymbol{\xi}, \quad q_i = \frac{1}{2} \int_{\mathbb{R}^3} |\boldsymbol{\xi} - \boldsymbol{u}|^2 (\xi_i - u_i) f \,\mathrm{d}\boldsymbol{\xi}, \quad i, j = 1, 2, 3. \tag{2.5}$$

For convenience, we define the pressure p and the stress tensor σ_{ij} by

$$p = \sum_{d=1}^{3} \frac{p_{dd}}{3} = \rho\theta, \quad \sigma_{ij} = p_{ij} - p\delta_{ij}, \quad i, j = 1, 2, 3.$$

2.2 The globally HME and its linearization

The moment method in kinetic theory is first proposed by Grad in 1949 [15]. Its primary idea is to expand the distribution function around the thermodynamic equilibrium into Hermite series

$$f(t, \boldsymbol{x}, \boldsymbol{\xi}) = \sum_{\alpha \in \mathbb{N}^3} f_\alpha(t, \boldsymbol{x}) \mathcal{H}_\alpha^{[\boldsymbol{u}, \theta]}(\boldsymbol{\xi}), \tag{2.6}$$

where $\alpha = (\alpha_1, \alpha_2, \alpha_3) \in \mathbb{N}^3$ is a 3-dimensional index, and $\mathcal{H}_\alpha^{[\boldsymbol{u}, \theta]}(\boldsymbol{\xi})$ is the basis function defined by

$$\mathcal{H}_\alpha^{[\boldsymbol{u}, \theta]}(\boldsymbol{\xi}) = \frac{\mathcal{M}}{\rho} He_\alpha^{[\boldsymbol{u}, \theta]}(\boldsymbol{\xi}). \tag{2.7}$$

where $He_\alpha^{[\boldsymbol{u}, \theta]}(\boldsymbol{\xi})$ is the generalized Hermite polynomial defined by

$$He_\alpha^{[\boldsymbol{u}, \theta]}(\boldsymbol{\xi}) = \frac{(-1)^{|\alpha|}}{\mathcal{M}} \frac{\partial^{|\alpha|} \mathcal{M}}{\partial \xi_1^{\alpha_1} \partial \xi_2^{\alpha_2} \partial \xi_3^{\alpha_3}}, \qquad |\alpha| := \sum_{d=1}^{3} \alpha_d. \tag{2.8}$$

The expansion coefficients f_α in (2.6) are related to the distribution function f by [7]

$$f_\alpha = \frac{\theta^{|\alpha|}}{\alpha!} \int_{\mathbb{R}^3} f He_\alpha^{[\boldsymbol{u}, \theta]}(\boldsymbol{\xi}) \,\mathrm{d}\boldsymbol{\xi}, \qquad \alpha! := \prod_{d=1}^{D} \alpha_d!. \tag{2.9}$$

Direct calculations yield, for $i, j = 1, 2, 3$,

$$f_0 = \rho, \quad f_{e_i} = 0, \quad \sum_{d=1}^{3} f_{2e_d} = 0, \quad \sigma_{ij} = (1 + \delta_{ij}) f_{e_i + e_j}, \tag{2.10}$$

where δ_{ij} is Kronecker delta and e_d, $d = 1, 2, 3$ is the d-th unit 3-dimensional index, with its d-th component to be the only nonzero one and equals to 1. Note that

$$Q(f) = -\frac{p}{\mu} \sum_{\alpha} \mathrm{H}(|\alpha| - 2) f_\alpha \mathcal{H}_\alpha^{[\boldsymbol{u}, \theta]}(\boldsymbol{\xi}), \qquad \mathrm{H}(n) = \begin{cases} 0, & n < 0, \\ 1, & n \geq 0. \end{cases}$$

Substituting Grad's expansion (2.6) into the Boltzmann equation, and matching coefficients of the basis function $\mathcal{H}_\alpha^{[\boldsymbol{u},\theta]}(\boldsymbol{\xi})$, one can obtain the governing equations of $\boldsymbol{u}$, θ and f_α, $\alpha \in \mathbb{N}^3$. However, the resulting system contains infinite number of equations. Choosing a positive integer $M \geq 3$, and discarding all the equations including $\dfrac{\partial f_\alpha}{\partial t}$, $|\alpha| > M$, then setting $f_\alpha = 0$, $|\alpha| > M$ to closure the residual system, we can obtain the M-th order Grad's moment system.

As pointed out in [35, 6], Grad's moment system lacks global hyperbolicity and is not hyperbolic even in any neighborhood of the thermodynamic equilibrium. The globally hyperbolic regularization proposed in [4, 5] figures the drawback out, and results in the globally Hyperbolic Moment Equations (HME) as: for any $|\alpha| \leq M$,

$$\begin{aligned}
&\frac{\mathrm{D}f_\alpha}{\mathrm{D}t} + \sum_{d=1}^{3}\left(\theta\frac{\partial f_{\alpha-e_d}}{\partial x_d} + (1-\delta_{|\alpha|,M})(\alpha_d+1)\frac{\partial f_{\alpha+e_d}}{\partial x_d}\right)\\
&+\sum_{k=1}^{3} f_{\alpha-e_k}\frac{\mathrm{D}u_k}{\mathrm{D}t} + \sum_{k,d=1}^{3}\frac{\partial u_k}{\partial x_d}\left(\theta f_{\alpha-e_k-e_d} + (1-\delta_{|\alpha|,M})(\alpha_d+1)f_{\alpha-e_k+e_d}\right)\\
&+\frac{1}{2}\sum_{k=1}^{3} f_{\alpha-2e_k}\frac{\mathrm{D}\theta}{\mathrm{D}t} + \sum_{k,d=1}^{3}\frac{1}{2}\frac{\partial\theta}{\partial x_d}\left(\theta f_{\alpha-2e_k-e_d} + (1-\delta_{|\alpha|,M})(\alpha_d+1)f_{\alpha-2e_k+e_d}\right) = -\frac{p}{\mu}f_\alpha \mathrm{H}(|\alpha|-2).
\end{aligned} \tag{2.11}$$

Here and hereafter we agree that $(\cdot)_\alpha$ is taken as zero if any component of α is negative.

Next, we try to derive the linearized system of (2.11). This requires us to examine the case that the distribution function is in a small neighborhood of an equilibrium state

$$\mathcal{M}_0(\boldsymbol{\xi}) = \frac{\rho_0}{(2\pi\theta_0)^{\frac{3}{2}}}\exp\left(-\frac{|\boldsymbol{\xi}|^2}{2\theta_0}\right),$$

given by $\rho_0, \boldsymbol{u}_0 = 0, \theta_0$. We introduce the dimensionless variables $\bar\rho$, $\bar{\boldsymbol{u}}$, $\bar\theta$, $\bar p$, $\bar p_{ij}$, $\bar f_\alpha$ and $\bar\mu$ as

$$\begin{aligned}
&\rho = \rho_0(1+\bar\rho), \quad \boldsymbol{u} = \sqrt{\theta_0}\bar{\boldsymbol{u}}, \quad \theta = \theta_0(1+\bar\theta), \quad p = p_0(1+\bar p),\\
&p_{ij} = p_0(\delta_{ij}+\bar p_{ij}), \quad f_\alpha = \rho_0\theta_0^{\frac{|\alpha|}{2}}\cdot\bar f_\alpha, \quad \mu = \mu_0(1+\bar\mu), \quad \boldsymbol{x} = L\cdot\bar{\boldsymbol{x}}, \quad t = \frac{L}{\sqrt{\theta_0}}\bar t,
\end{aligned} \tag{2.12}$$

where L is a characteristic length, $\bar{\boldsymbol{x}}$ and $\bar t$ are the dimensionless coordinates and time, respectively. We assume that all the dimensionless variables $\bar\rho$, $\bar{\boldsymbol{u}}$, $\bar\theta$, $\bar p$, $\bar p_{ij}$, $\bar f_\alpha$ and $\bar\mu$ are small quantities. Substituting (2.12) into the globally HME (2.11), and discarding all the small quantities of a higher order. Noticing that $u_d\dfrac{\partial\cdot}{\partial x_d}$ is small quantity of a higher order, $\dfrac{\mathrm{D}\cdot}{\mathrm{D}t} \approx \dfrac{\partial\cdot}{\partial\bar t}$, we obtain the linearized HME as

$$\begin{aligned}
&\frac{\partial\bar\rho}{\partial\bar t} + \sum_{d=1}^{3}\frac{\partial\bar u_d}{\partial\bar x_d} = 0,\\
&\frac{\partial\bar u_k}{\partial\bar t} + \frac{\partial\bar p}{\partial\bar x_k} + \sum_{d=1}^{3}\frac{\partial\bar\sigma_{kd}}{\partial\bar x_d} = 0,\\
&\frac{\partial\bar p_{ij}}{\partial\bar t} + \sum_{d=1}^{3}\delta_{ij}\frac{\partial\bar u_d}{\partial\bar x_d} + \frac{\partial\bar u_j}{\partial\bar x_i} + \frac{\partial\bar u_i}{\partial\bar x_j} + \sum_{d=1}^{3}(e_i+e_j+e_d)!\frac{\partial\bar f_{e_i+e_j+e_d}}{\partial\bar x_d} = -\frac{\bar\sigma_{ij}}{\mathrm{Kn}},\\
&\frac{\partial\bar f_\alpha}{\partial\bar t} + \sum_{d=1}^{3}\frac{\partial\bar f_{\alpha-e_d}}{\partial\bar x_d} + \sum_{d=1}^{3}(\alpha_d+1)(1-\delta_M)\frac{\partial\bar f_{\alpha+e_d}}{\partial\bar x_d} + \sum_{d=1}^{3}\frac{1}{2}\delta_{\alpha,e_d+2e_k}\frac{\partial\bar\theta}{\partial\bar x_d} = -\frac{\bar f_\alpha}{\mathrm{Kn}}, \quad 3 \leq |\alpha| \leq M,
\end{aligned} \tag{2.13}$$

where $\bar\sigma_{ij} = \bar p_{ij} - \bar p\delta_{ij}$, $i,j = 1,2,3$, and δ_{α,e_d+2e_k} is 1 iff $\alpha = e_d + 2e_k$. Here we define the Knudsen number Kn by

$$\mathrm{Kn} = \frac{\lambda}{L}, \tag{2.14}$$

where $\lambda = \frac{\mu_0}{p_0}\sqrt{\theta_0}$ is the mean free path.

3 Boundary Condition

In this paper, we adopt Maxwell's accommodation boundary condition [33], which is the most commonly used boundary condition in gas kinetic theory. It is formulated as a linear combination of the specular reflection and the diffuse reflection. For a point $\boldsymbol{x}$ at the wall, set the velocity and temperature of the wall as $\boldsymbol{u}^W(\boldsymbol{x})$ and $\theta^W(\boldsymbol{x})$, respectively. The theory of the hyperbolic problem indicates that the boundary conditions have to be imposed for $\boldsymbol{C}^W \cdot \boldsymbol{n} > 0$, where $\boldsymbol{C}^W = \boldsymbol{\xi} - \boldsymbol{u}^W$ and $\boldsymbol{n}$ is the unit normal vector pointing into the gas. The Maxwell's accommodation boundary condition reads

$$f^W(\boldsymbol{x}, \boldsymbol{\xi}) = \begin{cases} \chi \mathcal{M}^W(\boldsymbol{x}, \boldsymbol{\xi}) + (1-\chi) f(\boldsymbol{x}, \boldsymbol{\xi}^*), & \boldsymbol{C}^W \cdot \boldsymbol{n} > 0, \\ f(\boldsymbol{x}, \boldsymbol{\xi}), & \boldsymbol{C}^W \cdot \boldsymbol{n} \le 0, \end{cases} \tag{3.1}$$

where $\chi \in [0, 1]$ is the accommodation coefficient and

$$\boldsymbol{\xi}^* = \boldsymbol{\xi} - 2\left(\boldsymbol{C}^W \cdot \boldsymbol{n}\right)\boldsymbol{n}, \quad \mathcal{M}^W(\boldsymbol{x}, \boldsymbol{\xi}) = \frac{\rho^W(\boldsymbol{x})}{\left(2\pi\theta^W(\boldsymbol{x})\right)^{3/2}} \exp\left(-\frac{|\boldsymbol{C}^W(\boldsymbol{x}, \boldsymbol{\xi})|^2}{2\theta^W(\boldsymbol{x})}\right). \tag{3.2}$$

A boundary condition for the globally HME is proposed in [8], which is derived from the Maxwell boundary condition by calculating expression of the moments at the wall. Purposely considering steady shear flow, we adopt an alternative approach to derive our boundary conditions. Without loss of generality, let the unit normal vector of the wall $\boldsymbol{n} = (0, 1, 0)^T$, the velocity of the wall $\boldsymbol{u}^W = (u^W, 0, 0)$ and the velocity for steady shear flow $\boldsymbol{u} = (u_1, 0, 0)$. Taking them into (3.2) gives $\boldsymbol{\xi}^* = (\xi_1, -\xi_2, \xi_3)$. Thus (3.1) can be simplified as

$$f^W(\boldsymbol{x}, \boldsymbol{\xi}) = \begin{cases} \chi \mathcal{M}^W(\boldsymbol{x}, \boldsymbol{\xi}) + (1-\chi) f(\boldsymbol{x}, \boldsymbol{\xi}^*), & \xi_2 > 0, \\ f(\boldsymbol{x}, \boldsymbol{\xi}), & \xi_2 \le 0. \end{cases} \tag{3.3}$$

Denote $\Omega = \{\boldsymbol{\xi} \in \mathbb{R}^3\}$, $\Omega^+ = \{\xi_1 \in \mathbb{R}, \xi_2 \in \mathbb{R}^+, \xi_3 \in \mathbb{R}\}$ and $\Omega^- = \{\xi_1 \in \mathbb{R}, \xi_2 \in \mathbb{R}^-, \xi_3 \in \mathbb{R}\}$. The integral of the wall distribution function (3.3) with any function $\psi(\boldsymbol{C})$, $\boldsymbol{C} = (\xi_1 - u_1, \xi_2, \xi_3)$ gives us an equation

$$\int_\Omega \psi(\boldsymbol{C}) f^W(\boldsymbol{x}, \boldsymbol{\xi}) \, \mathrm{d}\boldsymbol{\xi} = \int_{\Omega^-} \psi(\boldsymbol{C}) f(\boldsymbol{x}, \boldsymbol{\xi}) \, \mathrm{d}\boldsymbol{\xi} + \int_{\Omega^+} \psi(\boldsymbol{C}) \left(\chi \mathcal{M}^W(\boldsymbol{x}, \boldsymbol{\xi}) + (1-\chi) f(\boldsymbol{x}, \boldsymbol{\xi}^*)\right) \mathrm{d}\boldsymbol{\xi}. \tag{3.4}$$

Definitely, for the globally HME one has to restrict the form of function $\psi(\boldsymbol{C})$, otherwise (3.4) will produce too many boundary conditions. It is clear that we should restrict ourselves to those ψ's that the moments in the equation can be retrieved. Thus those ψ's are polynomials as $\boldsymbol{C}^\beta$, where $\beta = (\beta_1, \beta_2, \beta_3) \in \mathbb{N}^3$ is a 3-dimensional multi-index and $|\beta| \le M$. Moreover, the distribution function of shear flow is an even function in the ξ_3 direction, which leads to $f_\beta = 0$, if β_3 is odd. Follow Grad's theory [15] to limit the number of boundary condition in order to ensure the continuity of boundary conditions when $\chi \to 0$, so only a subset of all the moments corresponding to

$$\{\boldsymbol{C}^\beta \big| \beta \in \mathbb{I}\}, \qquad \text{where} \qquad \mathbb{I} = \{|\beta| \le M \;\big|\; \beta_2 \text{ is odd and } \beta_3 \text{ is even}\} \tag{3.5}$$

are employed to construct the wall boundary conditions. Then we reformulate the equation (3.4) as

$$\int_{\Omega^+} \boldsymbol{C}^\beta \mathcal{M}^W(\boldsymbol{x}, \boldsymbol{\xi}) \, \mathrm{d}\boldsymbol{\xi} = \frac{1}{\chi}\left(\int_{\Omega^+} \boldsymbol{C}^\beta \left(f(\boldsymbol{x}, \boldsymbol{\xi}) - (1-\chi) f(\boldsymbol{x}, \boldsymbol{\xi}^*)\right) \mathrm{d}\boldsymbol{\xi}\right), \quad \beta \in \mathbb{I}. \tag{3.6}$$

Next we simplify (3.6) to derive the boundary condition for the HME. Note that the basis function (2.7) is decoupled in components of $\boldsymbol{\xi}$, and

$$\frac{1}{\sqrt{2\pi}} \int_0^{+\infty} \xi^k \exp\left(-\frac{|\xi|^2}{2}\right) \mathrm{d}\xi = \frac{2^{k/2-1}}{\sqrt{\pi}} \Gamma\left(\frac{k+1}{2}\right), \quad k \in \mathbb{N},$$

where $\Gamma(x)$ is the Gamma function. To simplify (3.6), we introduce the following notations

$$J_k(u,\theta) := \frac{1}{\sqrt{2\pi\theta}} \int_{\mathbb{R}} \xi^k \exp\left(-\frac{|\xi-u|^2}{2\theta}\right) \mathrm{d}\xi, \quad k \in \mathbb{N}, \tag{3.7a}$$

$$K(k,j) := \frac{1}{\sqrt{2\pi}} \int_{\mathbb{R}} \xi^k He_j(\xi) \exp\left(-\frac{|\xi|^2}{2}\right) \mathrm{d}\xi, \quad k,j \in \mathbb{N}, \tag{3.7b}$$

$$S(k,j) := \begin{cases} S^\star(k,j), & j \text{ is even}, \\ \dfrac{2-\chi}{\chi} S^\star(k,j), & j \text{ is odd}, \end{cases} \tag{3.7c}$$

where

$$S^\star(k,j) := \frac{1}{\sqrt{2\pi}} \int_0^{+\infty} \xi^k He_j(\xi) \exp\left(-\frac{\xi^2}{2}\right) \mathrm{d}\xi, \quad k,j \in \mathbb{N}, \tag{3.8}$$

and $He_j(\xi)$ is the j-th Hermite polynomial. Substituting (2.6) into (3.6), we can simplify the both hand sides of (3.6) as

$$\begin{aligned} \text{lhs of (3.6)} &= \frac{\rho^W \left(\theta^W\right)^{(\beta_2+\beta_3)/2}}{\sqrt{2\pi}} J_{\beta_1}\left(u_1^W - u_1, \theta^W\right) (\beta_2-1)!!(\beta_3-1)!!, \\ \text{rhs of (3.6)} &= \sum_{\alpha\in\mathbb{N}^3} \left(K(\beta_1,\alpha_1) S(\beta_2,\alpha_2) K(\beta_3,\alpha_3) \theta^{(\beta_2-\alpha_2)/2}\right) f_\alpha. \end{aligned} \tag{3.9}$$

The orthogonality of Hermite polynomials indicates $K(0,j) = \delta_{0,j}$, so by setting $\beta = e_2$ in (3.9), we have

$$\rho^W \sqrt{\frac{\theta^W}{2\pi}} = \sum_{j=0}^{\infty} S(1,j) \frac{f_{je_2}}{\theta^{(j-1)/2}}.$$

Note that $S(k,0) = \dfrac{1}{\sqrt{2\pi}}(k-1)!!$, if k is odd. The boundary condition for the case $\beta = e_1 + \beta_2 e_2 \in \mathbb{I}$ in (3.5) is

$$S(\beta_2,0)\rho^W \left(\theta^W\right)^{\frac{\beta_2}{2}} \left(u_1^W - u_1\right) = \sum_{\alpha_2} S(\beta_2,\alpha_2) f_{e_1+\alpha_2 e_2} \theta^{(\beta_2-\alpha_2)/2}. \tag{3.10}$$

We linearize the boundary conditions at θ_0 as that in (2.12) for our purpose, and assume $\theta^W - \theta_0$ is a small quantity. Substituting (2.12) into (3.10) and applying the closure of the HME, i.e. $f_\alpha = 0$, $|\alpha| > M$, the linearized boundary condition is arrived as

$$S(\beta_2,0)(\bar{u}_1^W - \bar{u}_1) = \sum_{\alpha_2=1}^{M-1} S(\beta_2,\alpha_2) \bar{f}_{e_1+\alpha_2 e_2}, \tag{3.11}$$

where $\bar{u}_1^W$ is defined as dimensionless variable $u_1^W = \sqrt{\theta_0}\bar{u}_1^W$, and β_2 is odd and $\beta_2 < M$.

Before the end of this section, we list some properties of $S^\star(k,j)$ in (3.8) for later usage.

Property 1. *The coefficients $S^\star(k,j)$ satisfy the following relationships:*

1. *Recursion relation:*

$$S^\star(k,j) = (k-1)S^\star(k-2,j) + jS^\star(k-1,j-1), \quad k,j \in \mathbb{N}, k \geq 1. \tag{3.12}$$

2. *The value of $S^\star(k,j)$ is:*

   - *If $j \leq k$:*

$$\begin{aligned} &\text{if } k-j \text{ is even, } S^\star(k,j) = A_1; \\ &\text{if } k-j \text{ is odd, } S^\star(k,j) = \frac{1}{\sqrt{2\pi}} \cdot A_2. \end{aligned} \tag{3.13}$$

     Here A_1 and A_2 are both algebraic numbers.
   - *If $j > k$ and $k-j$ is even, $S^\star(k,j) = 0$.*

The proof of the property is provided in Appendix A.

4 Kramers' Problem

We focus on the analytical solution of the linearized HME for the Kramers' problem in this section. The setup for Kramers' problem is standard. The gas flow in a half-space over a flat wall is considered, where the coordinate is chosen such that x direction is parallel to the wall, and y direction is perpendicular to the wall. The solid wall is fixed on $\bar{y} = 0$ ($\bar{u}_1^W = 0$), both temperature and density of the gas far from the wall are constant. Gas velocity $\bar{\boldsymbol{u}} = (\bar{u}_1, 0, 0)$ and all derivatives in equations (2.13) in x and z direction vanish. Since Kramers' problem is a half-space problem, the characteristic length L is not defined, which indicates the Knudsen number is not well-defined. Noticing Kramers' problem aims at the solution with respect to y/λ, we set the Knudsen number as $\mathrm{Kn} = 1$ hereafter.

4.1 Formal solution of the linearized HME

In this subsection, we try to explore the formal solution of the linearized HME. The setup of Kramers' problem makes equations of the linearized HME (2.13) related to velocity decoupled from the whole linearized HME, which enables us to investigate the velocity by studying a small system as

$$\begin{aligned}
\frac{\mathrm{d}\bar{\sigma}_{12}(\bar{y})}{\mathrm{d}\bar{y}} &= 0,\\
\frac{\mathrm{d}\bar{u}_1(\bar{y})}{\mathrm{d}\bar{y}} + 2\frac{\mathrm{d}\bar{f}_{e_1+2e_2}(\bar{y})}{\mathrm{d}\bar{y}} &= -\bar{\sigma}_{12}(\bar{y}),\\
\frac{\mathrm{d}\bar{\sigma}_{12}(\bar{y})}{\mathrm{d}\bar{y}} + 3\frac{\mathrm{d}\bar{f}_{e_1+3e_2}(\bar{y})}{\mathrm{d}\bar{y}} &= -\bar{f}_{e_1+2e_2}(\bar{y}),\\
&\cdots\\
\frac{\mathrm{d}\bar{f}_{e_1+(M-2)e_2}(\bar{y})}{\mathrm{d}\bar{y}} &= -\bar{f}_{e_1+(M-1)e_2}(\bar{y}),
\end{aligned} \tag{4.1}$$

with the boundary condition

$$S(k,0)\bar{u}_1(0) + \sum_{j=1}^{M-1} S(k,j)\bar{f}_{e_1+je_2}(0) = 0, \quad k \text{ is odd and } k < M. \tag{4.2}$$

We collect the variables involved in (4.1) into a vector

$$V(\bar{y}) = \left(\bar{u}_1(\bar{y}), \bar{\sigma}_{12}(\bar{y}), \bar{f}_{e_1+2e_2}(\bar{y}), \bar{f}_{e_1+3e_2}(\bar{y}), \cdots, \bar{f}_{e_1+(M-1)e_2}(\bar{y})\right)^T,$$

then the subsystem (4.1) can be reformulated as

$$\mathbf{M}\frac{\mathrm{d}V(\bar{y})}{\mathrm{d}\bar{y}} = -\mathbf{Q}V(\bar{y}), \tag{4.3}$$

with the boundary condition

$$\mathbf{B}V(0) = 0, \tag{4.4}$$

where

$$\mathbf{M} = \begin{pmatrix}
0 & 1 & & & & \\
1 & 0 & 2 & & & \\
 & 1 & 0 & 3 & & \\
 & & \ddots & \ddots & \ddots & \\
 & & & 1 & 0 & M-1\\
 & & & & 1 & 0
\end{pmatrix}_{M\times M}, \quad \mathbf{Q} = \begin{pmatrix}
0 & & & \\
 & 1 & & \\
 & & \ddots & \\
 & & & 1
\end{pmatrix}_{M\times M}, \tag{4.5}$$

and $\mathbf{B} = (b_{ij})_{m\times M}$ with $b_{ij} = S(2i-1, j-1)$. Here we define $m = \lfloor \frac{M}{2} \rfloor$. One can easily check that the matrix $\mathbf{M}$ is real diagonalizable. Precisely, there exists an eigen-decomposition of $\mathbf{M}$ as $\mathbf{M} = \mathbf{R}\mathbf{\Lambda}\mathbf{R}^{-1}$, where

$\mathbf{R}$ is the Hermite transformation matrix

$$\mathbf{R} = (r_{ij})_{M\times M}, \quad r_{ij} = \frac{He_{i-1}(\lambda_j)}{(i-1)!}, \quad i,j = 1,\cdots,M, \tag{4.6}$$

and $\mathbf{\Lambda} = \mathrm{diag}\{\lambda_i; i = 1,\cdots,M\}$. Here the eigenvalue λ_i, $i = 1,\cdots,M$ is the i-th largest zero of the M-th order Hermite polynomial $He_M(x)$. Since $\lambda_i > 0$, $i = 1,\cdots,m$ and $\lambda_i \le 0$, $i = m+1,\cdots,M$, we can write the diagonal matrix $\mathbf{\Lambda}$ as

$$\mathbf{\Lambda} = \begin{pmatrix} \mathbf{\Lambda}_+ & \\ & \mathbf{\Lambda}_{\le 0} \end{pmatrix}, \tag{4.7}$$

$$\mathbf{\Lambda}_+ = \mathrm{diag}\left\{\lambda_i;\ i = 1,\cdots,m\right\}, \quad \mathbf{\Lambda}_{\le 0} = \mathrm{diag}\left\{\lambda_i;\ i = m+1,\cdots,M\right\}. \tag{4.8}$$

The first equation of (4.3) indicates $\bar{\sigma}_{12}$ is a constant and the second equation of (4.3) gives that

$$\bar{u}_1(\bar{y}) = -\bar{\sigma}_{12}\bar{y} - 2\bar{f}_{e_1+2e_2}(\bar{y}) + c_0, \tag{4.9}$$

where c_0 is a constant to be determined. Let

$$\hat{V}(\bar{y}) = \left(\bar{f}_{e_1+2e_2}(\bar{y}), \bar{f}_{e_1+3e_2}(\bar{y}), \cdots, \bar{f}_{e_1+(M-1)e_2}(\bar{y})\right)^T,$$

which is the remaining part of $V(\bar{y})$ excluded the first two variables $\bar{u}_1(\bar{y})$ and $\bar{\sigma}_{12}(\bar{y})$. Then the governing equations of $\hat{V}(\bar{y})$ can be deduced from (4.3) as

$$\hat{\mathbf{M}}\frac{\mathrm{d}\hat{V}(\bar{y})}{\mathrm{d}\bar{y}} = -\hat{V}(\bar{y}), \tag{4.10}$$

where

$$\hat{\mathbf{M}} = \begin{pmatrix} 0 & 3 & & & & \\ 1 & 0 & 4 & & & \\ & 1 & 0 & 5 & & \\ & & \ddots & \ddots & \ddots & \\ & & & 1 & 0 & M-1 \\ & & & & 1 & 0 \end{pmatrix}.$$

Similarly as the matrix $\mathbf{M}$, the matrix $\hat{\mathbf{M}}$ is also real diagonalizable. Precisely, let

$$\hat{He}_0(x) = 1,\ \hat{He}_1(x) = x,\ \hat{He}_{k+1}(x) = x\hat{He}_k(x) - (k+2)\hat{He}_{k-1}(x),\ k \ge 1,$$

then the characteristic polynomial of $\hat{\mathbf{M}}$ is $\hat{He}_{M-2}(\lambda)$. The recursion relation implies that $\hat{He}_k(x)$ has k real and simple zeros, thus $\hat{\mathbf{M}}$ is real diagonalizable and its eigenvalue $\hat{\lambda}_i$ is the i-th largest zero of $\hat{He}_{M-2}(\lambda)$. Furthermore, if $\hat{\lambda}_i$ is an eigenvalue of $\hat{\mathbf{M}}$, then $-\hat{\lambda}_i$ has to be an eigenvalue of $\hat{\mathbf{M}}$, since $\hat{He}_{M-2}(x)$ is an odd function if M is odd and is an even function if M is even. Similarly as $\mathbf{\Lambda}$ in (4.7), we split the matrix $\hat{\mathbf{\Lambda}}$ as

$$\hat{\mathbf{\Lambda}} = \begin{pmatrix} \hat{\mathbf{\Lambda}}_+ & \\ & \hat{\mathbf{\Lambda}}_{\le 0} \end{pmatrix},$$

$$\hat{\mathbf{\Lambda}}_+ = \mathrm{diag}\left\{\hat{\lambda}_i;\ i = 1,\cdots,m-1\right\}, \quad \hat{\mathbf{\Lambda}}_{\le 0} = \mathrm{diag}\left\{\hat{\lambda}_i;\ i = m,\cdots,M-2\right\}.$$

The matrix $\hat{\mathbf{M}}$ can be decomposed as $\hat{\mathbf{M}} = \hat{\mathbf{R}}\hat{\mathbf{\Lambda}}\hat{\mathbf{R}}^{-1}$, where

$$\hat{\mathbf{R}} = (\hat{r}_{ij})_{(M-2)\times(M-2)}, \quad \hat{r}_{ij} = \frac{\hat{He}_{i-1}(\hat{\lambda}_j)}{(i+1)!}, \quad i,j = 1,\cdots,M-2. \tag{4.11}$$

4.1.1 Illustrative examples: $M \le 5$

We examine the cases for small M to find out the formal solution for generic M.

M=3 This is the simplest system. For this case, $\bar{f}_{e_1+2e_2}(\bar{y}) = -\dfrac{\mathrm{d}\bar{\sigma}_{12}(\bar{y})}{\mathrm{d}\bar{y}} = 0$, so the solution of the velocity profile is

$$\bar{u}_1(\bar{y}) = -\bar{\sigma}_{12}\bar{y} + c_0.$$

It is clear that the solution of $\bar{u}_1(\bar{y})$ is not able to capture the Knudsen layer because $\bar{u}_1$ is a linear function of $\bar{y}$. In order to capture the Knudsen layer of velocity, we need more moments and higher order moment equations.

M=4 Here the variables $\hat{V}(\bar{y}) = \left(\bar{f}_{e_1+2e_2}(\bar{y}), \bar{f}_{e_1+3e_2}(\bar{y})\right)^T$ and

$$\hat{\mathbf{M}} = \begin{pmatrix} 0 & 3 \\ 1 & 0 \end{pmatrix}, \tag{4.12}$$

which can be decomposed as $\hat{\mathbf{M}} = \hat{\mathbf{R}}\hat{\mathbf{\Lambda}}\hat{\mathbf{R}}^{-1}$ with

$$\hat{\mathbf{\Lambda}} = \begin{pmatrix} \sqrt{3} & \\ & -\sqrt{3} \end{pmatrix}, \quad \hat{\mathbf{R}} = \begin{pmatrix} 1 & 1 \\ \frac{1}{\sqrt{3}} & -\frac{1}{\sqrt{3}} \end{pmatrix}.$$

Hence, the solution of system (4.10) is

$$\hat{V}(\bar{y}) = \hat{\mathbf{R}} \exp\left(-\hat{\mathbf{\Lambda}}^{-1}\bar{y}\right) \hat{\mathbf{R}}^{-1}\hat{V}(0).$$

By setting $\hat{\boldsymbol{c}} = (\hat{c}_1, \hat{c}_2)^T = \hat{\mathbf{R}}^{-1}\hat{V}(0)$, we have

$$\hat{V}(\bar{y}) = \begin{pmatrix} \bar{f}_{e_1+2e_2}(\bar{y}) \\ \bar{f}_{e_1+3e_2}(\bar{y}) \end{pmatrix} = \hat{\mathbf{R}} \exp\left(-\hat{\mathbf{\Lambda}}^{-1}\bar{y}\right) \hat{\boldsymbol{c}} = \begin{pmatrix} \hat{c}_1 \exp(-\frac{\bar{y}}{\sqrt{3}}) + \hat{c}_2 \exp(\frac{\bar{y}}{\sqrt{3}}) \\ \frac{\sqrt{3}}{3}\hat{c}_1 \exp(-\frac{\bar{y}}{\sqrt{3}}) - \frac{\sqrt{3}}{3}\hat{c}_2 \exp(\frac{\bar{y}}{\sqrt{3}}) \end{pmatrix}.$$

The exponential terms provide the Knudsen layer. Since all the variables have to remain finite as $\bar{y} \to \infty$, the term $\exp(\bar{y}/\sqrt{3})$ has to be dropped, i.e.

$$\begin{pmatrix} \bar{f}_{e_1+2e_2}(\bar{y}) \\ \bar{f}_{e_1+3e_2}(\bar{y}) \end{pmatrix} = \hat{\mathbf{R}} \begin{pmatrix} \exp\left(-\hat{\mathbf{\Lambda}}_+^{-1}\bar{y}\right) & \\ & \mathbf{0} \end{pmatrix} \hat{\boldsymbol{c}} = \hat{c}_1 \exp\left(-\frac{\bar{y}}{\sqrt{3}}\right) \begin{pmatrix} 1 \\ \frac{\sqrt{3}}{3} \end{pmatrix}.$$

Here $\hat{\mathbf{\Lambda}}_+$ is a 1×1 matrix with its entry $\sqrt{3}$. By taking (4.9) into the linearized boundary condition (4.2), i.e.

$$\begin{aligned} S(1,0)\bar{u}_1(0) + S(1,1)\bar{\sigma}_{12}(0) + S(1,2)\bar{f}_{e_1+2e_2}(0) + S(1,3)\bar{f}_{e_1+3e_2}(0) = 0, \\ S(3,0)\bar{u}_1(0) + S(3,1)\bar{\sigma}_{12}(0) + S(3,2)\bar{f}_{e_1+2e_2}(0) + S(3,3)\bar{f}_{e_1+3e_2}(0) = 0, \end{aligned}$$

we can obtain

$$\begin{pmatrix} S(1,0) & S(1,2) + \frac{\sqrt{3}}{3}S(1,3) - 2S(1,0) \\ S(3,0) & S(3,2) + \frac{\sqrt{3}}{3}S(3,3) - 2S(3,0) \end{pmatrix} \begin{pmatrix} c_0 \\ \hat{c}_1 \end{pmatrix} = -\bar{\sigma}_{12} \begin{pmatrix} S(1,1) \\ S(3,1) \end{pmatrix}.$$

Direct calculations yield

$$\hat{c}_1 = \frac{1}{2}\frac{\sqrt{2\pi}(\chi-2)}{\sqrt{6\pi}\chi - 4\chi - 2\sqrt{6\pi}}\bar{\sigma}_{12}, \quad c_0 = -\frac{1}{2}\frac{\sqrt{\pi}(\chi-2)\left(2\sqrt{3\pi}\chi - 5\sqrt{2}\chi - 4\sqrt{3\pi}\right)}{\left(\sqrt{6\pi}\chi - 4\chi - 2\sqrt{6\pi}\right)\chi}\bar{\sigma}_{12},$$

and the solution of the velocity profile

$$\bar{u}_1(\bar{y}) = -\bar{\sigma}_{12}\bar{y} - 2\hat{c}_1 \exp\left(-\frac{\bar{y}}{\sqrt{3}}\right) + c_0.$$

M=5 For this case, $\hat{V}(\bar{y}) = \left(\bar{f}_{e_1+2e_2}(\bar{y}), \bar{f}_{e_1+3e_2}(\bar{y}), \bar{f}_{e_1+4e_2}(\bar{y})\right)^T$, and the matrix $\hat{\mathbf{M}} = \hat{\mathbf{R}}\hat{\mathbf{\Lambda}}\hat{\mathbf{R}}^{-1}$ in (4.10) is

$$\hat{\mathbf{M}} = \begin{pmatrix} 0 & 3 & 0 \\ 1 & 0 & 4 \\ 0 & 1 & 0 \end{pmatrix} \text{ with } \hat{\mathbf{\Lambda}} = \begin{pmatrix} \sqrt{7} & & \\ & 0 & \\ & & -\sqrt{7} \end{pmatrix}, \quad \hat{\mathbf{R}} = \begin{pmatrix} 1 & 1 & 1 \\ \sqrt{7}/3 & 0 & -\sqrt{7}/3 \\ 1/3 & -1/4 & 1/3 \end{pmatrix}.$$

Note that $M = 5$ is odd, so zero is a simple eigenvalue of $\hat{\mathbf{M}}$. This vanished eigenvalue provides a constant factor in the exponential terms for the Knudsen layer, while the eigenvalue $\sqrt{7}$ of matrix $\hat{\mathbf{M}}$ provides the only stable term which survives in the solution. The solution of (4.10) is

$$\hat{V}(\bar{y}) = \begin{pmatrix} \bar{f}_{e_1+2e_2}(\bar{y}) \\ \bar{f}_{e_1+3e_2}(\bar{y}) \\ \bar{f}_{e_1+4e_2}(\bar{y}) \end{pmatrix} = \hat{\mathbf{R}} \begin{pmatrix} \exp\left(-\hat{\mathbf{\Lambda}}_+^{-1}\bar{y}\right) & \\ & \mathbf{0} \end{pmatrix} \hat{\boldsymbol{c}} = \hat{c}_1 \exp\left(-\frac{\bar{y}}{\sqrt{7}}\right) \begin{pmatrix} 1 \\ \sqrt{7}/3 \\ 1/3 \end{pmatrix},$$

where $\hat{\boldsymbol{c}} = (\hat{c}_1, \hat{c}_2, \hat{c}_3)^T = \hat{\mathbf{R}}^{-1}\hat{V}(0)$ and the entry of the 1×1 matrix $\hat{\mathbf{\Lambda}}_+$ is $\sqrt{7}$. Similarly as the case $M = 4$, there are 2 coefficients c_0 and $\hat{c}_1$ to be determined. By taking (4.9) into the linearized boundary condition (4.2), i.e.

$$\begin{aligned} &S(1,0)\bar{u}_1(0) + S(1,1)\bar{\sigma}_{12}(0) + S(1,2)\bar{f}_{e_1+2e_2}(0) + S(1,3)\bar{f}_{e_1+3e_2}(0) + S(1,4)\bar{f}_{e_1+4e_2}(0) = 0, \\ &S(3,0)\bar{u}_1(0) + S(3,1)\bar{\sigma}_{12}(0) + S(3,2)\bar{f}_{e_1+2e_2}(0) + S(3,3)\bar{f}_{e_1+3e_2}(0) + S(3,4)\bar{f}_{e_1+4e_2}(0) = 0, \end{aligned}$$

we can obtain

$$\begin{pmatrix} S(1,0) & S(1,2) + \frac{\sqrt{7}}{3}S(1,3) + \frac{1}{3}S(1,4) - 2S(1,0) \\ S(3,0) & S(3,2) + \frac{\sqrt{7}}{3}S(3,3) + \frac{1}{3}S(3,4) - 2S(3,0) \end{pmatrix} \begin{pmatrix} c_0 \\ \hat{c}_1 \end{pmatrix} = -\bar{\sigma}_{12} \begin{pmatrix} S(1,1) \\ S(3,1) \end{pmatrix}.$$

Direct calculations yield

$$\hat{c}_1 = \frac{3\sqrt{2\pi}(\chi - 2)}{2\left(3\sqrt{14\pi}\chi - 20\chi - 6\sqrt{14\pi}\right)}\bar{\sigma}_{12}, \quad c_0 = \frac{3\sqrt{\pi}(2-\chi)}{\chi}\left(\frac{\sqrt{7\pi}\chi - 4\sqrt{2}\chi - 2\sqrt{7\pi}}{3\sqrt{14\pi}\chi - 20\chi - 6\sqrt{14\pi}}\right)\bar{\sigma}_{12},$$

and the solution of the velocity profile

$$\bar{u}_1(\bar{y}) = -\bar{\sigma}_{12}\bar{y} - 2\hat{c}_1 \exp\left(-\frac{\bar{y}}{\sqrt{7}}\right) + c_0.$$

4.1.2 General case: arbitrary M

Now we are ready to present the formal solution of the velocity profile for arbitrary M. Following the examples above, we have to drop those unbounded terms to attain a stable solution that only the terms contributed from the positive eigenvalues of $\hat{\mathbf{M}}$ are kept. Thus the stable solution of (4.10) is

$$\hat{V}(\bar{y}) = \hat{\mathbf{R}} \begin{pmatrix} \exp\left(-\hat{\mathbf{\Lambda}}_+^{-1}\bar{y}\right) & \\ & \mathbf{0} \end{pmatrix} \hat{\boldsymbol{c}}, \tag{4.13}$$

where $\hat{\boldsymbol{c}} = (\hat{c}_1, \cdots, \hat{c}_{M-2})^T = \hat{\mathbf{R}}^{-1}\hat{V}(0)$. Clearly, only the first $m-1$ entries in $\hat{\boldsymbol{c}}$ appear in $\hat{V}(\bar{y})$. With the expression of $\bar{f}_{e_1+2e_2}(\bar{y})$ provided as the first entry of $\hat{V}(\bar{y})$, the velocity is given by the second equation in (4.1) as

$$\begin{aligned} \bar{u}_1(\bar{y}) &= -\bar{\sigma}_{12}\bar{y} - 2\boldsymbol{e}_1^T\hat{V}(\bar{y}) + c_0 \\ &= -\bar{\sigma}_{12}\bar{y} - 2\boldsymbol{e}_1^T\hat{\mathbf{R}} \begin{pmatrix} \exp\left(-\hat{\mathbf{\Lambda}}_+^{-1}\bar{y}\right) & \\ & \mathbf{0} \end{pmatrix} \hat{\boldsymbol{c}} + c_0 \\ &= -\bar{\sigma}_{12}\bar{y} - 2\sum_{i=1}^{m-1} \hat{c}_i \exp\left(-\frac{\bar{y}}{\hat{\lambda}_i}\right) + c_0, \end{aligned} \tag{4.14}$$

where $\boldsymbol{e}_1 = (1, 0, \cdots, 0)^T$. Since c_0 in the expression of $\bar{u}_1(\bar{y})$ is also to be determined, there are in total m indeterminate coefficients in $V(\bar{y})$. Once these coefficients are fixed by the boundary conditions, we eventually attain the general formula for the $\bar{u}_1(\bar{y})$.

Noticing the linearized boundary condition (4.2), i.e. for $k = 1, \ldots, m$,

$$\{\mathbf{B}V(0)\}_k = S(2k-1,0)\bar{u}_1(0) + S(2k-1,1)\bar{\sigma}_{12}(0) + \sum_{j=2}^{M-1} S(2k-1,j)\bar{f}_{e_1+je_2}(0) = 0,$$

and $\bar{u}_1(0) = -2\sum_{i=1}^{m-1}\hat{c}_i + c_0$, the linear system can be obtained as

$$\mathbf{A}\boldsymbol{c} = -\sigma_{12}\boldsymbol{b}, \tag{4.15}$$

where $\mathbf{A} = \left(\boldsymbol{h}, (\mathbf{S} - 2\boldsymbol{h}\boldsymbol{e}_1^T)\hat{\mathbf{R}}_+\right)$ and $\boldsymbol{c} = (c_0, \hat{c}_1, \cdots, \hat{c}_{m-1})^T$. Here the matrix $\hat{\mathbf{R}}_+$ is the left $m-1$ columns of $\hat{\mathbf{R}}$, i.e.

$$\hat{\mathbf{R}}_+ = \begin{pmatrix} \dfrac{\hat{H}e_0(\hat{\lambda}_1)}{2!} & \cdots & \dfrac{\hat{H}e_0(\hat{\lambda}_{m-1})}{2!} \\ \vdots & \ddots & \vdots \\ \dfrac{\hat{H}e_{M-3}(\hat{\lambda}_1)}{(M-1)!} & \cdots & \dfrac{\hat{H}e_{M-3}(\hat{\lambda}_{m-1})}{(M-1)!} \end{pmatrix},$$

and

$$\boldsymbol{h} = \begin{pmatrix} S(1,0) \\ S(3,0) \\ \vdots \\ S(2m-1,0) \end{pmatrix}, \qquad \boldsymbol{b} = \begin{pmatrix} S(1,1) \\ S(3,1) \\ \vdots \\ S(2m-1,1) \end{pmatrix},$$

$$\mathbf{S} = \begin{pmatrix} S(1,2) & S(1,3) & \cdots & S(1,M-1) \\ S(3,2) & S(3,3) & \cdots & S(3,M-1) \\ \vdots & \vdots & \ddots & \vdots \\ S(2m-1,2) & S(2m-1,3) & \cdots & S(2m-1,M-1) \end{pmatrix}.$$

4.2 Unique solvability of linearized HME for Kramers' problem

To obtain the analytical solution of the velocity profile (4.14), one only need to solve the linear algebraic equations (4.15). Therefore, whether the linear system (4.15) is unique solvability concerns the unique solvability of the linearized HME. In the subsection, we study the unique solvability of the linear system and the following result are obtained.

Theorem 1. $|\mathbf{A}| \neq 0$ *if* $\dfrac{2-\chi}{\sqrt{2\pi\chi}}$ *is not an algebraic number.*

In order to prove Theorem 1, we define some symbols and introduce a Lemma first. Similarly as the definition of $\hat{\mathbf{R}}_+$, the right $M-m-1$ columns of $\hat{\mathbf{R}}$ is denoted by $\hat{\mathbf{R}}_-$. Let $\hat{\mathbf{R}}_{+,\text{even}}$, which is made with the even rows of $\hat{\mathbf{R}}_+$ as

$$\begin{aligned} \hat{\mathbf{R}}_{+,\text{even}} &\triangleq (\hat{r}_{ij}), \text{ where } i \text{ is even}, j = 1, \cdots, m-1, \\ &= \begin{pmatrix} \dfrac{\hat{H}e_1(\hat{\lambda}_1)}{3!} & \dfrac{\hat{H}e_1(\hat{\lambda}_2)}{3!} & \cdots & \dfrac{\hat{H}e_1(\hat{\lambda}_{m-1})}{3!} \\ \dfrac{\hat{H}e_3(\hat{\lambda}_1)}{5!} & \dfrac{\hat{H}e_3(\hat{\lambda}_2)}{5!} & \cdots & \dfrac{\hat{H}e_3(\hat{\lambda}_{m-1})}{5!} \\ \vdots & \vdots & \cdots & \vdots \end{pmatrix}, \end{aligned}$$

be a $m-1 \times m-1$ square matrix. Analogously, we define $\hat{\mathbf{R}}_{+,\text{odd}}, \hat{\mathbf{R}}_{-,\text{odd}}, \hat{\mathbf{R}}_{-,\text{odd}}$ as

$$\begin{aligned} \hat{\mathbf{R}}_{+,\text{odd}} &\triangleq (\hat{r}_{ij}), \text{ where } i \text{ is odd}, j = 1, \cdots, m-1, \\ \hat{\mathbf{R}}_{-,\text{even}} &\triangleq (\hat{r}_{ij}), \text{ where } i \text{ is even}, j = m, \cdots, M-2, \\ \hat{\mathbf{R}}_{-,\text{odd}} &\triangleq (\hat{r}_{ij}), \text{ where } i \text{ is odd}, j = m, \cdots, M-2. \end{aligned}$$

Lemma 1. $\hat{\mathbf{R}}_{+,even}$ *is invertible.*

Proof. Let $\mathbf{P}_\sigma$ be the permutation matrix given by the permutation

$$\sigma : \{1, 2, \cdots, M-2\} \to \{1, 2, \cdots, M-2\}, \tag{4.16}$$

which maps the list of numbers $1, 2, \cdots, M-2$ to

$$2, 4, 6, \cdots, 1, 3, 5, \cdots,$$

i.e. the even numbers are ahead of the odd numbers. Then matrix $\hat{\mathbf{R}}$ is re-organized by the permutation matrix as

$$\mathbf{P}_\sigma^{-1}\hat{\mathbf{R}} = \left(\begin{array}{c|c} \hat{\mathbf{R}}_{+,\text{even}} & \hat{\mathbf{R}}_{-,\text{even}} \\ \hat{\mathbf{R}}_{+,\text{odd}} & \hat{\mathbf{R}}_{-,\text{odd}} \end{array}\right).$$

Note that for each eigenvalue $\hat{\lambda}_i \in \hat{\mathbf{\Lambda}}_+$, we have $-\hat{\lambda}_i \in \hat{\mathbf{\Lambda}}_{\leq 0}$. Then for any eigenvector

$$\hat{\boldsymbol{r}}_i = (\hat{\boldsymbol{r}}_{i,\text{even}}|\hat{\boldsymbol{r}}_{i,\text{odd}})^T \in (\hat{\mathbf{R}}_{+,\text{even}}|\hat{\mathbf{R}}_{+,\text{odd}})^T,$$

there exists a column vector

$$\hat{\boldsymbol{r}}_j = (-\hat{\boldsymbol{r}}_{i,\text{even}}|\hat{\boldsymbol{r}}_{i,\text{odd}})^T \in (\hat{\mathbf{R}}_{-,\text{even}}|\hat{\mathbf{R}}_{-,\text{odd}})^T.$$

Then

$$\hat{\boldsymbol{r}}_i - \hat{\boldsymbol{r}}_j = 2(\hat{\boldsymbol{r}}_{i,\text{even}}|\mathbf{0})^T.$$

The set of vectors $\hat{\boldsymbol{r}}_i - \hat{\boldsymbol{r}}_j$ are linearly independent since $\hat{\boldsymbol{r}}_i, \hat{\boldsymbol{r}}_j$ are eigenvectors of $\hat{\mathbf{R}}$, then columns of $\hat{\mathbf{R}}_{+,\text{even}}$ are linearly independent. Thus $\hat{\mathbf{R}}_{+,\text{even}}$ is invertible. □

With the help of the upper Lemma, we can prove Theorem 1 now.

Proof of Theorem 1. Noticing $\mathbf{A}\begin{pmatrix} 1 & 2\boldsymbol{e}_1^T\hat{\mathbf{R}}_+ \\ \mathbf{0} & \mathbf{I} \end{pmatrix} = (\boldsymbol{h}, \mathbf{S}\hat{\mathbf{R}}_+)$, we have $|\mathbf{A}| = |(\boldsymbol{h}, \mathbf{S}\hat{\mathbf{R}}_+)|$. We retrieve the coefficient $h_j(\chi)$ in $S(k, j)$ and obtain

$$\mathbf{S} = \mathbf{S}_0^\star \mathbf{H},$$

where $\mathbf{H} = \text{diag}\{h_2(\chi), h_3(\chi), \cdots, h_{M-1}(\chi)\}$ and

$$\mathbf{S}_0^\star = \begin{pmatrix} S^\star(1,2) & S^\star(1,3) & \cdots & S^\star(1,M-1) \\ S^\star(3,2) & S^\star(3,3) & \cdots & S^\star(3,M-1) \\ \vdots & \vdots & \ddots & \vdots \\ S^\star(2m-1,2) & S^\star(2m-1,3) & \cdots & S^\star(2m-1,M-1) \end{pmatrix}.$$

By the recursion relation (3.12) of $S^\star(k, j)$, we have that

$$\mathbf{L}\mathbf{S}_0^\star = \begin{pmatrix} S^\star(1,2), & S^\star(1,3), & \cdots, & S^\star(1,M-1) \\ & & \mathbf{S}_1^\star & \end{pmatrix},$$

where

$$\mathbf{L} = \begin{pmatrix} 1 & & & & \\ -2 & 1 & & & \\ & -4 & 1 & & \\ & & \ddots & \ddots & \\ & & & -(2m-2) & 1 \end{pmatrix},$$

and

$$\mathbf{S}_1^\star = \begin{pmatrix} 2S^\star(2,1) & 3S^\star(2,2) & \cdots & (M-1)S^\star(2,M-2) \\ 2S^\star(4,1) & 3S^\star(4,2) & \cdots & (M-1)S^\star(4,M-2) \\ \vdots & \vdots & \ddots & \vdots \\ 2S^\star(2m-2,1) & 3S^\star(2m-2,2) & \cdots & (M-1)S^\star(2m-2,M-2) \end{pmatrix}.$$

Noticing that $\mathbf{L}\boldsymbol{h} = \left(1/\sqrt{2\pi}, 0, \cdots, 0\right)^T$, we have that

$$(\boldsymbol{h}, \mathbf{S}\hat{\mathbf{R}}_+) = \mathbf{L}^{-1} \begin{pmatrix} 1/\sqrt{2\pi} & (S^\star(1,2), \cdots, S^\star(1,M-1)) \\ \mathbf{0} & \mathbf{S}_1^\star \end{pmatrix} \begin{pmatrix} 1 & \\ & \mathbf{H}\hat{\mathbf{R}}_+ \end{pmatrix}.$$

Thus we just need to verify the determinant of $\mathbf{S}_1^\star \mathbf{H}\hat{\mathbf{R}}_+$ is not vanished. Considering the permutation matrix in (4.16), one gets

$$\mathbf{S}_1^\star \mathbf{P}_\sigma = (\mathbf{S}_{\text{even}}^\star, \mathbf{S}_2^\star),$$

where $\mathbf{S}_{\text{even}}^\star$ is made with the even columns of $\mathbf{S}_1^\star$ as

$$\mathbf{S}_{\text{even}}^\star = \begin{pmatrix} 3S^\star(2,2) & 5S^\star(2,4) & 7S^\star(2,6) & \dots \\ 3S^\star(4,2) & 5S^\star(4,4) & 7S^\star(4,6) & \dots \\ \vdots & \vdots & \vdots & \vdots \\ 3S^\star(2m-2,2) & 5S^\star(2m-2,4) & 7S^\star(2m-2,6) & \dots \end{pmatrix},$$

and $\mathbf{S}_2^\star$ is made with the odd columns of $\mathbf{S}_1^\star$ as

$$\mathbf{S}_2^\star := \frac{1}{\sqrt{2\pi}} \mathbf{S}_{\text{odd}}^\star = \begin{pmatrix} 2S^\star(2,1) & 4S^\star(2,3) & 6S^\star(2,5) & \dots \\ 2S^\star(4,1) & 4S^\star(4,3) & 6S^\star(2,5) & \dots \\ \vdots & \vdots & \vdots & \vdots \\ 2S^\star(2m-2,1) & 4S^\star(2m-2,3) & 6S^\star(2m-2,5) & \dots \end{pmatrix}.$$

With the integral properties of $S^\star(k,j)$ in (3.13), $\mathbf{S}_{\text{even}}^\star$ is a lower triangular matrix while each entry in matrices $\mathbf{S}_{\text{even}}^\star$ and $\mathbf{S}_{\text{odd}}^\star$ is an algebraic number.

The diagonal matrix $\mathbf{H}$ is turned into

$$\mathbf{P}_\sigma^{-1} \mathbf{H} \mathbf{P}_\sigma = \begin{pmatrix} \mathbf{I} & \\ & \dfrac{2-\chi}{\chi}\mathbf{I} \end{pmatrix}.$$

We then have that

$$\begin{aligned} \mathbf{S}_1^\star \mathbf{H}\hat{\mathbf{R}}_+ =& \mathbf{S}_1^\star \mathbf{P}_\sigma \ \mathbf{P}_\sigma^{-1} \mathbf{H} \mathbf{P}_\sigma \ \mathbf{P}_\sigma^{-1} \hat{\mathbf{R}}_+ \\ =& (\mathbf{S}_{\text{even}}^\star, \frac{1}{\sqrt{2\pi}} \mathbf{S}_{\text{odd}}^\star) \begin{pmatrix} \mathbf{I} & \\ & \dfrac{2-\chi}{\chi}\mathbf{I} \end{pmatrix} \begin{pmatrix} \hat{\mathbf{R}}_{+,\text{even}} \\ \hat{\mathbf{R}}_{+,\text{odd}} \end{pmatrix} \\ =& \mathbf{S}_{\text{even}}^\star \hat{\mathbf{R}}_{+,\text{even}} + \frac{2-\chi}{\sqrt{2\pi}\chi} \mathbf{S}_{\text{odd}}^\star \hat{\mathbf{R}}_{+,\text{odd}}. \end{aligned}$$

Since $\hat{\mathbf{R}}_{+,\text{even}}$ is invertible by Lemma 1,

$$\mathbf{S}_1^\star \mathbf{H}\hat{\mathbf{R}}_+ = \left(\mathbf{S}_{\text{even}}^\star + \frac{2-\chi}{\sqrt{2\pi}\chi} \mathbf{S}_{\text{odd}}^\star \hat{\mathbf{R}}_{+,\text{odd}} \hat{\mathbf{R}}_{+,\text{even}}^{-1} \right) \hat{\mathbf{R}}_{+,\text{even}}, \tag{4.17}$$

and we only need to verify the matrix $\mathbf{S}_{\text{even}}^\star + \dfrac{2-\chi}{\sqrt{2\pi}\chi} \mathbf{S}_{\text{odd}}^\star \hat{\mathbf{R}}_{+,\text{odd}} \hat{\mathbf{R}}_{+,\text{even}}^{-1}$ in (4.17) is not singular. Define the polynomial of x by

$$p(x) \triangleq \left| \mathbf{S}_{\text{even}}^\star + x \mathbf{S}_{\text{odd}}^\star \hat{\mathbf{R}}_{+,\text{odd}} \hat{\mathbf{R}}_{+,\text{even}}^{-1} \right|. \tag{4.18}$$

Since each entry of matrices $\mathbf{S}_{\text{even}}^\star$, $\hat{\mathbf{R}}_{+,\text{even}}^{-1}$, $\mathbf{S}_{\text{odd}}^\star$, and $\hat{\mathbf{R}}_{+,\text{odd}}$ is an algebraic number, all the coefficients of $p(x)$ are algebraic numbers. If x is a transcendental number, then $p(x) \neq 0$ [24], i.e. if $\dfrac{2-\chi}{\sqrt{2\pi}\chi}$ is not an algebraic number, $|\mathbf{A}| \neq 0$. This completes the proof. □

Remark 1. Noticing the set $\left\{\chi \in (0,1] \mid \dfrac{2-\chi}{\sqrt{2\pi}\chi} \text{ is an algebraic number}\right\}$ has Lebesgue measure zero, we prove that $|\mathbf{A}| \neq 0$ holds for almost all $\chi \in (0,1]$ in Theorem 1. Particularly, if χ is an algebraic number, then $\dfrac{2-\chi}{\sqrt{2\pi}\chi}$ is not an algebraic number. In practical applications, the accommodation coefficient χ is always an algebraic number. On the other hand, $p(x)$ in (4.18) is a polynomial with respect to x of degree $m-1$, so there are at most $m-1$ zeros of $p(x)$, which indicates there are at most $m-1$ $\chi \in (0,1]$ such that $|\mathbf{A}| = 0$.

Remark 2. Definitely, we speculate that $|\mathbf{A}| \neq 0$ for all $\chi \in (0,1]$, while unfortunately we can not prove it due to our limited knowledge on the number theory. However, with the help of computer algebra system in Maple [1], we have verified that $|\mathbf{A}| \neq 0$ for any $\chi \in (0,1]$ for M ranging from 3 to 100. Moreover, numerical investigation shows that all the coefficients of $p(x)$ are positive or negative, simultaneously, which support that $p(x)$ has no zeros in $\mathbb{R}^+$, thus $|\mathbf{A}| \neq 0$.

Theorem 1 is important for the well-posedness of the boundary condition (3.9) of linearized HME. As is well-known, for nonlinear hyperbolic equations, how to present a well-posed boundary condition is always an important and challenging issue. In gas kinetic theory, there are many works on the boundary condition for the moment equations[38, 41, 17, 8]. For the globally HME, the boundary condition is first proposed in [8], where the authors deduced the boundary condition from Maxwell's accommodation boundary condition by studying the moments of f^W in (3.1), which is the most natural choice to deduce the boundary condition for moment equations. However, it is still not clear whether the boundary condition is well-posed. Theorem 1 indicates in the sense of linearization, the boundary condition is well-posed for the plane problem because the solution is uniquely determined if the accommodation coefficient χ satisfies that $\dfrac{2-\chi}{\sqrt{2\pi}\chi}$ is not an algebraic number.

5 Quantitative Verification of Knudsen Layer

In this section, we quantitatively study the velocity profile in the Knudsen layer. In order to avoid numerical error, high precision computation is used in all the tests.

To be consistent with the kinetic solutions obtained from the Boltzmann equation, the velocity in (4.14) can be normalized as

$$\tilde{u}(\bar{y}) = -\frac{\bar{u}}{\bar{\sigma}_{12}} = \bar{y} + \frac{1}{\bar{\sigma}_{12}}\left(2\sum_{i=1}^{m-1}\hat{c}_i \exp\left(-\frac{\bar{y}}{\hat{\lambda}_i}\right) - c_0\right). \tag{5.1}$$

The normalized velocity can be split into three parts [42, 37]: the linear part $\bar{y}$, the slip coefficient ζ and the velocity defect $\tilde{u}_d(\bar{y})$

$$\tilde{u}(\bar{y}) = \bar{y} + \zeta - \tilde{u}_d(\bar{y}). \tag{5.2}$$

Here the velocity defect $\tilde{u}_d(\bar{y})$ is defined by

$$\tilde{u}_d(\bar{y}) = -2\sum_{i=1}^{m-1}\frac{\hat{c}_i}{\bar{\sigma}_{12}} \exp\left(-\frac{\bar{y}}{\hat{\lambda}_i}\right), \tag{5.3}$$

satisfying $\lim\limits_{\bar{y}\to+\infty} \tilde{u}_d(\bar{y}) = 0$; ζ is the slip coefficient, defined by

$$\zeta = \lim_{\bar{y}\to+\infty}(\tilde{u}(\bar{y}) + \tilde{u}_d(\bar{y}) - \bar{y}) = -\frac{c_0}{\bar{\sigma}_{12}}. \tag{5.4}$$

They are often used to study how the wall affects the velocity profile [37, 17]. Note that there always exists a factor $\bar{\sigma}_{12}$ in the expression of $\hat{c}_i$ and c_0 in (4.14).

5.1 Normalized velocity

In this subsection, we quantitatively examine the velocity profile by investigating the normalized velocity (5.1), the velocity defect (5.3) and the effective viscosity, which is an important parameter to describe the non-Newtonian behaviour inherent in the Kramers' problem.

[1] Maple is a trademark of Waterloo Maple Inc.

Normalized velocity Fig. 5.1 present the profile of $\tilde{u}(\bar{y})$ in (5.1) of the linearized HME with $M = 8$ and $M = 9$. Compared with numerical results of the linearized Boltzmann-BGK equation in [31], a good agreement of the solutions of the linearized HME in Fig. 5.1 indicates the moment system with a small M is good enough to describe the velocity profile in the Knudsen layer. Moreover, the value of $\tilde{u}(\bar{y})$ increases, as χ decreasing. This is because the coefficients $\hat{c}_i$ and c_0 are dependent on $(2-\chi)/\chi$. As the definition of χ in Section 3, the diffusion interaction between gas and the wall is weaker for smaller χ.

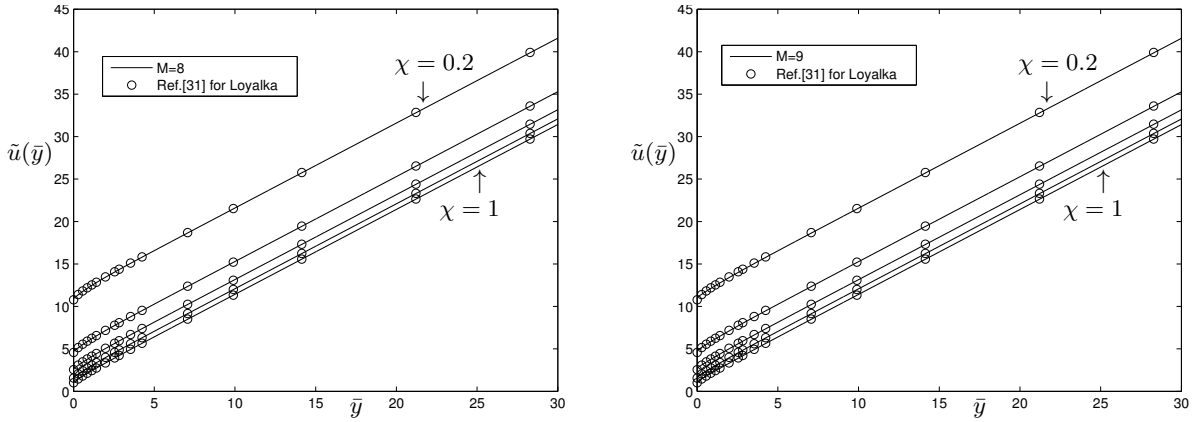

(a) $M = 8$ (b) $M = 9$

Figure 5.1: Profile of $\tilde{u}(\bar{y})$ of the linearized HME for different accommodation number χ and different M. The reference solution is Loyalka's result in [31]. In each figure, the lines from up to down correspond to $\chi = 0.2, 0.4, 0.6, 0.8, 1$, respectively.

Velocity defect Velocity defect, which is in the form of superpositions of exponential functions, is usually used to study the Knudsen layer. Fig. 5.2 presents the profile of defect velocity for the linearized HME with $M = 8$ and $M = 9$, the results of R26 in [17], and the results of the linearized Boltzmann-BGK equation [29]. One can find that the result of linearized HME has a better agreement with [29] beyond $\bar{y} = 1$, for the analytical result consists of 4 exponential parts, which preserve more kinetic information. Meanwhile, we find that the three moment models predict a relative smaller velocity defect than the numerical result [29] close to the wall. It is expected that more moments are required to describe the Knudsen layer when $\bar{y} \to 0$, which will be studied in details in the next subsection.

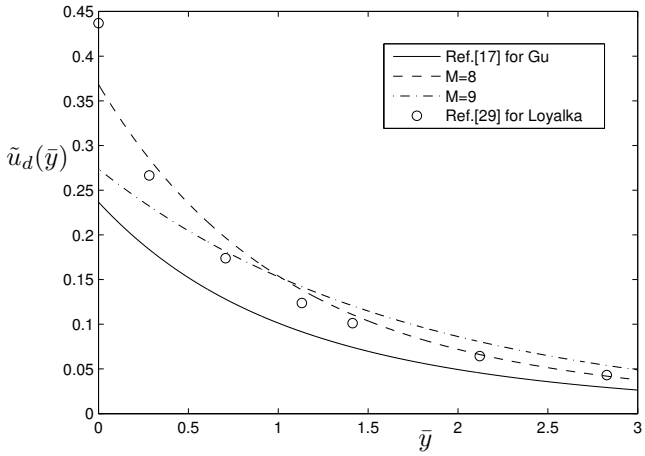

Figure 5.2: Profile of the defect velocity $\tilde{u}_d(\bar{y})$ of the linearized HME for $M = 8$ and $M = 9$ with $\chi = 1$. The reference solution is Loyalka's result in [29] for linearized Boltzmann-BGK model.

Effective viscosity Effective viscosity is an important quantity to describe the non-Newtonian behavior inherent in the Kramers' problem. As we know, the Navier-Stokes law indicates $\sigma_{12} = -\mu_0 \dfrac{\partial u}{\partial y}$ while the continuum assumption is valid. However, the Navier-Stokes law fails in the Knudsen layer. To describe the non-Newtonian behavior inherent in the Knudsen layer, we formally write the Navier-Stokes law on the shear stress σ_{12} as

$$\sigma_{12} = -\mu_{\text{eff}} \frac{\partial u}{\partial y}, \tag{5.5}$$

where μ_{eff} is called the effective viscosity. Since the shear stress σ_{12} is constant in the Kramers' problem, we have

$$\frac{\mu_{\text{eff}}}{\mu_0} = -\left(\frac{\sigma_{12}}{\partial u/\partial y}\right) \Big/ \left(\frac{\lambda p_0}{\sqrt{\theta_0}}\right) = -\frac{\bar{\sigma}_{12}}{\partial \bar{u}/\partial \bar{y}} = \frac{1}{\partial \tilde{u}/\partial \bar{y}}. \tag{5.6}$$

Noticing the definition of the normalized velocity (5.1), one can directly obtain

$$\mu_{\text{eff}} = \frac{\mu_0}{1 + \sum_{i=1}^{m-1} c_i \exp\left(-\bar{y}/\hat{\lambda}_i\right)}, \quad c_i = -\frac{2\hat{c}_i}{\hat{\lambda}_i \bar{\sigma}_{12}}. \tag{5.7}$$

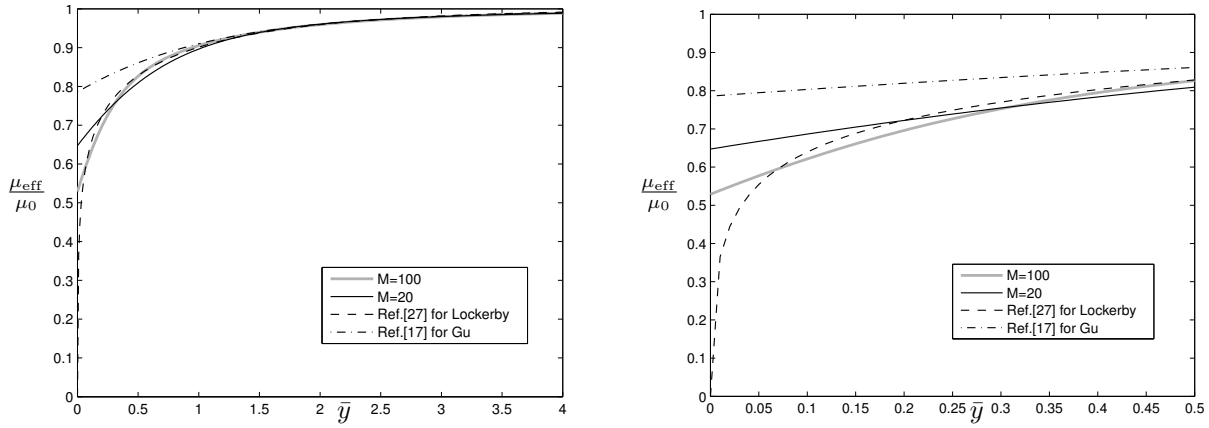

(a) large scale (b) small scale

Figure 5.3: Effective viscosity μ_{eff} with different kinetic model.

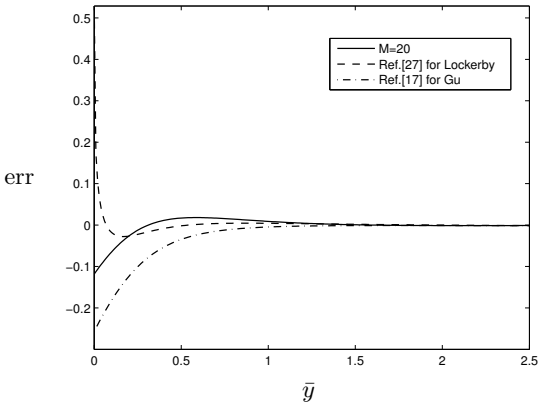

Figure 5.4: Comparison between effective viscosity μ_{eff} with different kinetic model.

The effective viscosity is well studied in the literatures. For example, Gu [17] investigated the R26 moment equations and predicted the effective viscosity as

$$\mu_{\text{eff}} = \left(1 - \left(1.3042C_1 \exp\left(-1.265\bar{y}\right) + 1.6751C_2 \exp\left(-0.5102\bar{y}\right)\right)\right)^{-1} \mu_0, \tag{5.8}$$

where

$$C_1 = \frac{\chi - 2}{\chi} \frac{0.81265 \times 10^{-1}\chi^2 + 1.2824\chi}{0.48517 \times 10^{-2}\chi^2 + 0.64884\chi + 8.0995},$$
$$C_2 = \frac{\chi - 2}{\chi} \frac{0.8565 \times 10^{-3}\chi^2 + 0.362\chi}{0.48517 \times 10^{-2}\chi^2 + 0.64884\chi + 8.0995}.$$

This model is similar as the linearized HME. Actually, since R26 moment system can be derived from the globally HME, Gu's result can be regarded as a special case of the linearized HME.

In [27], Lockerby et al. studied the effective viscosity based on the two low-Kn BGK results, and proposed an empirical expression as

$$\mu_{\text{eff}} = \left(1 + 0.1859\left(\sqrt{\frac{2}{\pi}}\bar{y}\right)^{-0.464} \exp\left(-0.7902\left(\sqrt{\frac{2}{\pi}}\bar{y}\right)\right)\right)^{-1} \mu_0. \tag{5.9}$$

For Lockerby's model, we have $\mu_{\text{eff}} \to 0$ as $\bar{y} \to 0+$, which indicates the velocity gradient to approach infinity at the wall. (Here (5.8) and (5.9) are converted to be consistent with the present value of the Knudsen number.)

Fig. 5.3 shows the profile of the effective viscosity of these models. Here we take the solution of the linearized HME with $M = 100$ as the reference solution. One can observe that Gu gives a relatively larger effective viscosity μ_{eff}, while Lockerby gives a relatively smaller one. If one wants to obtain a good approximation of the effective viscosity close to the wall, many moments are demanded.

We also take the solution of the linearized HME with $M = 100$ as the reference solution, and define the error as

$$\text{err} = \mu_{\text{eff}}^{\text{reference}} - \mu_{\text{eff}}^{\text{model}}.$$

Fig. 5.4 shows the error of Gu's and Lockerby's models and the linearized HME with $M = 20$. Gu's model agrees with the reference very well away from the Knudsen layer and gives too large effective viscosity, while Lockerby's model gives too small effective viscosity. For the linearized HME, by choosing a proper M, the effective viscosity can be well captured.

5.2 Quantitative Verification in moment order

As shown in Section 5.1, we need more moments to describe the Knudsen layer when $\bar{y} \to 0$. Here we quantitatively study the solution of the velocity defect and slip coefficient of the linearized HME, respectively, as the moment order M increases.

Before we compared analytical solutions of the linearized HME with numerical solution of the linearized Boltzmann-BGK equation in this section, we first introduce the linearized Boltzmann-BGK equation for Kramers' problem in [42]. The author writes the distribution function as

$$f(\boldsymbol{x}, \boldsymbol{\xi}) = \mathcal{M}(\boldsymbol{x}, \boldsymbol{\xi})[1 + h(\boldsymbol{x}, \boldsymbol{\xi})], \tag{5.10}$$

where $h(\boldsymbol{x}, \boldsymbol{\xi})$ is a disturbance term caused by the small perturbation near the local equilibrium $\mathcal{M}(\boldsymbol{x}, \boldsymbol{\xi})$, which has the form

$$\mathcal{M}(\boldsymbol{x}, \boldsymbol{\xi}) = \frac{\rho_0(x, y)}{(2\pi\theta_0(x, y))^{3/2}} \exp\left(-\frac{(\xi_x - Ky)^2 + \xi_y^2 + \xi_z^2}{2\theta_0(x, y)}\right),$$

where ρ_0 and θ_0 are the same as that in (2.12), and K is taken as a constant $-\dfrac{\sigma_{12}}{\mu_0}$ for Kramers' problem. Substituting (5.10) into the Boltzmann equation (2.1), discarding the high-order terms and applying the

standard setup of Kramers' problem, we obtain the dimensionless linearized Boltzmann-BGK equation for Kramers' problem as

$$K_0\bar{\xi}+\bar{\xi}\frac{\partial Z(\bar{y},\bar{\xi})}{\partial \bar{y}}=-Z(\bar{y},\bar{\xi})+\frac{1}{\sqrt{2\pi}}\int_{\mathbb{R}} Z(\bar{y},\bar{\xi}')\exp\left(-\frac{\bar{\xi}'^2}{2}\right)\,\mathrm{d}\bar{\xi}', \tag{5.11}$$

with the boundary condition

$$Z(0,\bar{\xi})=(1-\chi)Z(0,-\bar{\xi}),\quad \xi>0. \tag{5.12}$$

Here $\bar{y}$ is the dimensionless variable same as that in (2.12), $\boldsymbol{\xi}=\sqrt{\theta_0}\bar{\boldsymbol{\xi}}$, $K_0=LK/\sqrt{\theta_0}$, and $Z(\bar{y},\bar{\xi})$ is related to $h(\boldsymbol{x},\boldsymbol{\xi})$ by

$$Z(\bar{y},\bar{\xi})=\frac{1}{2\pi}\int_{\mathbb{R}^2} h\left(\lambda\bar{y},\sqrt{\theta_0}\bar{\boldsymbol{\xi}}\right)\bar{\xi}_x\exp\left(-\frac{\bar{\xi}_x^2+\bar{\xi}_z^2}{2}\right)\,\mathrm{d}\bar{\xi}_x\,\mathrm{d}\bar{\xi}_z, \tag{5.13}$$

where λ is defined by (2.14).

We point out that the linearized HME (4.1) and its boundary condition (4.2) for Kramers' problem can be regarded as a discretization of the linearized Boltzmann-BGK equation (5.11) with its boundary condition (5.12), together with the Gauss-Hermite quadrature in the velocity space (see Appendix B for more details). Therefore, it is expected that the analytical results of the linearized HME will have a good agreement with that of the linearized Boltzmann-BGK equation as M increases. In Section 5.1, we have shown that the velocity profile of the linearized HME has a close agreement with that of the linearized Boltzmann-BGK equation (5.11). Next, we quantitatively verify the solution of the velocity defect and slip coefficient of the linearized HME, respectively, as M increases.

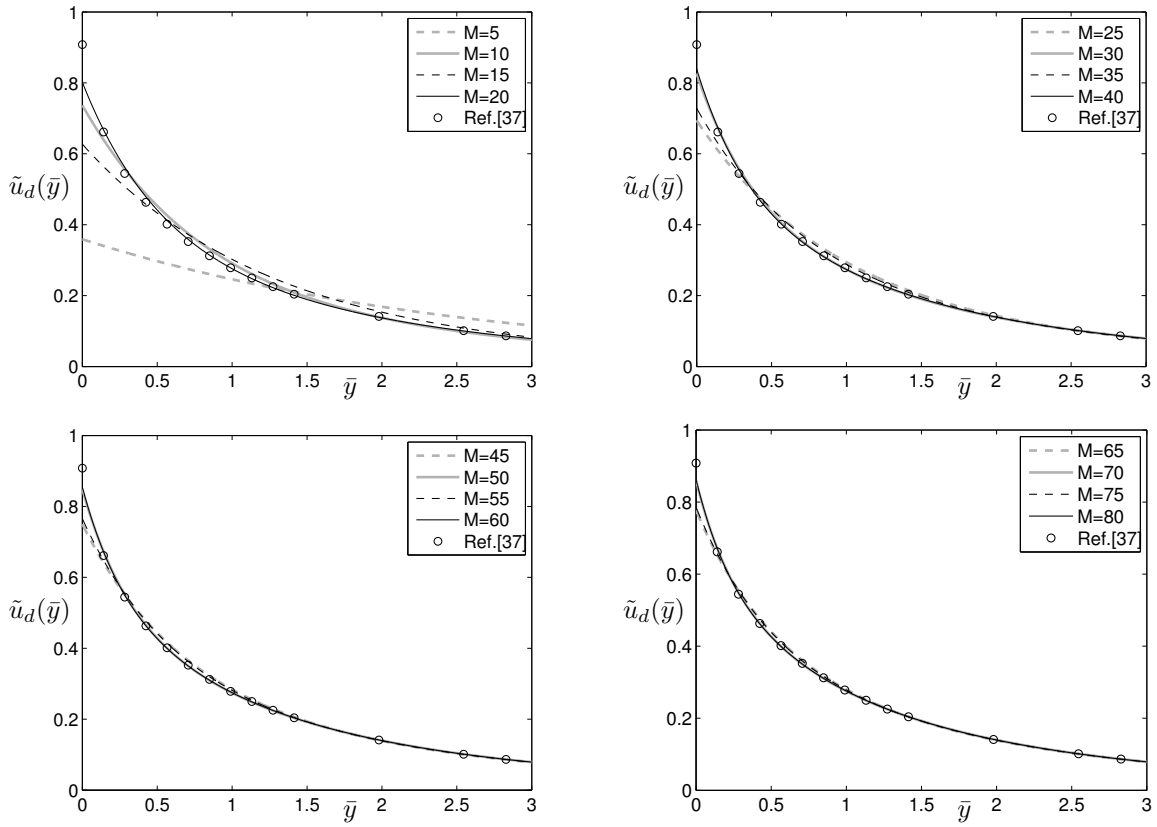

Figure 5.5: Profile of the defect velocity $\tilde{u}_d(\bar{y})$ of the linearized HME for different M with $\chi=0.1$. The reference solution is Siewert's result in [37] for linearized Boltzmann-BGK model.

For the velocity defect $\tilde{u}_d(\bar{y})$ in (5.3), the analytical results with M ranging from 5 to 80 are presented in Fig. 5.5 for $\chi=0.1$ and Fig. 5.6 for $\chi=0.9$. The reference solution is the Siewert's numerical results

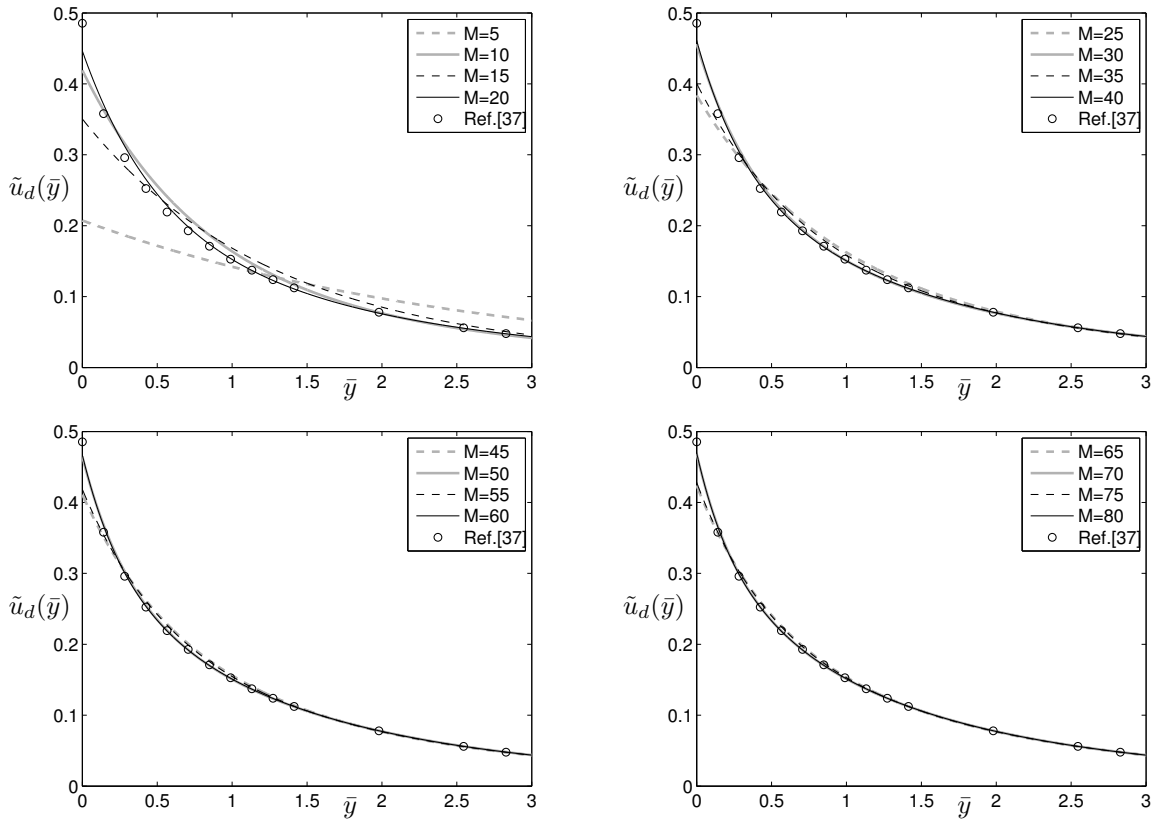

Figure 5.6: Profile of the defect velocity $\tilde{u}_d(\bar{y})$ of the linearized HME for different M with $\chi = 0.9$. The reference solution is Siewert's result in [37] for linearized Boltzmann-BGK model.

in [37] for the linearized Boltzmann-BGK model. Clearly, the results of the linearized HME have a better agreement to Siewert's result as M increases, which is consistent with the theoretical analysis in Sec. 5.2. Meanwhile, one can find that the defect velocity of even order approaches faster to the reference solution than that of odd order. This can be understood based on the smallest width of the Knudsen layer, which is represented by $w_M := \min\{\hat{\lambda}_i : i = 1, \cdots, m-1\}$. The smaller w_M, the closer of the defect velocity of the linearized HME to the reference solution. Fig. 5.7 gives all the $\hat{\lambda}_i$ for M ranging from 3 to 40. One can observe that w_M for even M is quite less than that for the adjacent odd M.

Moreover, comparing with Fig. 5.5 and 5.6, one can find that for a given M, the relative error in Fig. 5.5 is a little greater than that of Fig. 5.6. Actually, for smaller χ, the diffusion interaction between the gas and the wall turns weak, then the distribution function is expected to be farther from the equilibrium, which indicates more moments are needed.

For the slip coefficient ζ, the analytical results for different M are plotted in Fig. 5.8. Similar trend can be readily observed in Fig. 5.8. All the conclusion for Fig. 5.5 and 5.6 hold for Fig. 5.8.

In the quantitative study for the solution of the linearized HME, we observe that the linearized HME can capture the profile of all the slip coefficient ζ, the velocity defect $\tilde{u}_d$ and the effective viscosity very well for any accommodation coefficient χ. For the slip coefficient, when M up to 18, the relative error between the linearized HME and the reference result is less than 3‰. For the velocity defect, we obtain a good agreement with the reference solution, even for $M = 8$. Moreover, the linearized HME gives a good approximation of the effective viscosity for not very large M, for example, $M = 20$. These indicate that in practical numerical simulations, we normally don't need to use too many moments. $M = 18$ is good enough for almost all the cases, and $M \leq 10$ might be good enough for most cases. Note that the number of moments is $N = M + 1$ for 1D and $N = \dfrac{(M+1)(M+2)(M+3)}{6}$ for 3D, and the computational cost of the numerical scheme for

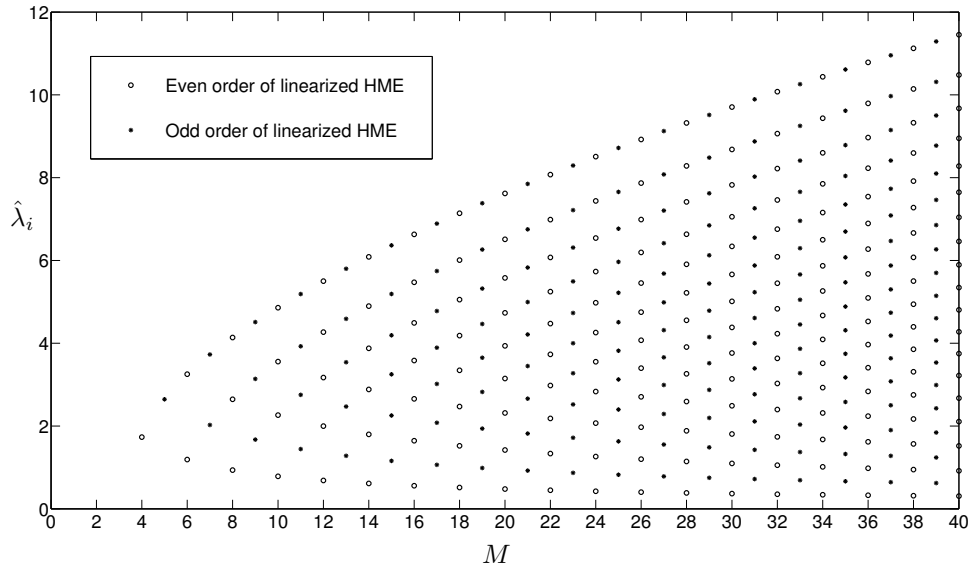

Figure 5.7: The value $\hat{\lambda}_i$ for different M.

HME [9, 7] is $O(N_x N)$, where N_x is the number of discrete points in space. If we set $M = 10$, there are only 286 equations in the moment system, which is acceptable for numerical simulations.

6 Conclusion

In this paper, we use linearized HME to study the Kramers' problem. With the help of the linearization, we presented the analytical solution of the linearized HME and proved that the solution is unique. The defect velocity and slip coefficient are well studied in comparison of the existing models and the numerical solution of linearized Boltzmann-BGK equation. By comparing with the velocity profile of the linearized Boltzmann-BGK equation, we showed that the linearized HME captures the Knudsen layer velocity profile over a wide range of accommodation coefficients accurately with not too many moments, which indicates that the physics of non-equilibrium gas flow can be captured by the linearized HME.

7 Acknowledgement

We thank the anonymous referees for their valuable comments and suggestions on the paper. The research of J. Li is partially supported by the Hong Kong Research Council ECS grant No. 509213 during her visit periods at the Hong Kong Polytechnic University. The research of J. Li and R. Li are supported by the National Natural Science Foundation of China (11325102, 11421110001, 91630310). The research of Z.-H. Qiao is partially supported by the Hong Kong Research Council ECS grant No. 509213 and the Hong Kong Polytechnic University research fund G-YBKP.

Appendix

A Proof of Property 1

Proof of Property 1. We first review some properties of Hermite polynomials as follows:

- Recursion relation: $He_{j+1}(x) = xHe_j(x) - jHe_{j-1}(x)$;
- Differential relation: $[He_j(x)\exp(-x^2/2)]' = -He_{j+1}(x)\exp(-x^2/2)$.

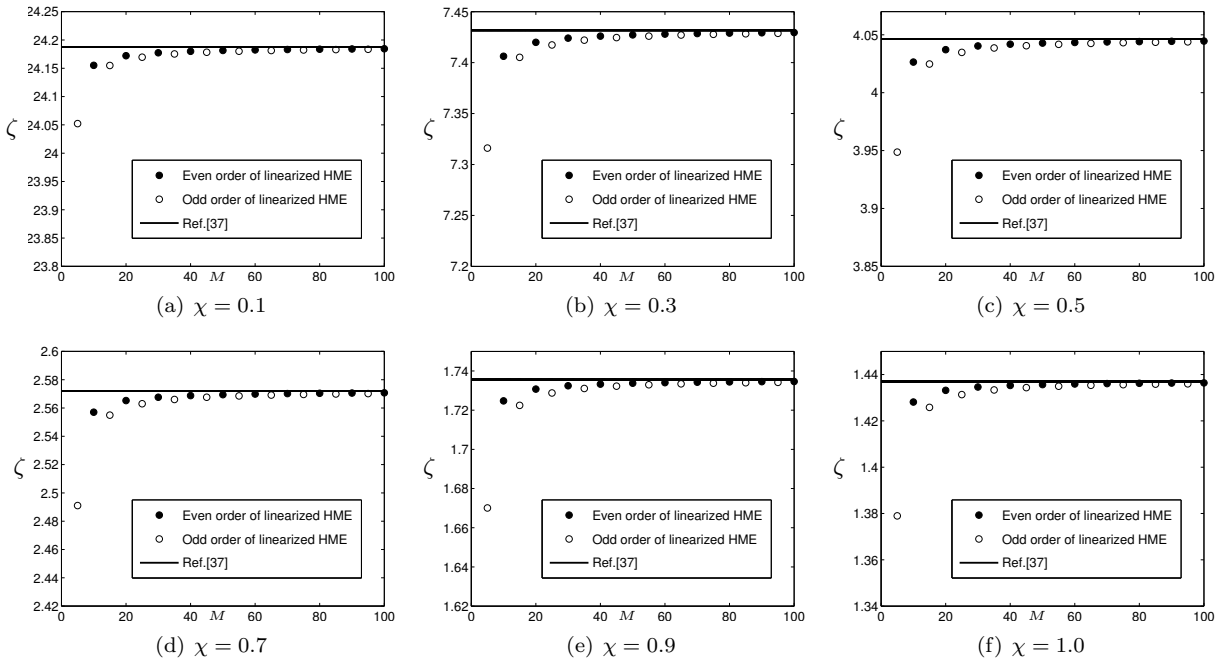

(a) $\chi = 0.1$ (b) $\chi = 0.3$ (c) $\chi = 0.5$

(d) $\chi = 0.7$ (e) $\chi = 0.9$ (f) $\chi = 1.0$

Figure 5.8: Values of the slip coefficient ζ for different M and χ. The reference solution is Siewert's result in [37] for linearized BGK model.

It can be easily seen that (3.12) holds for $k = 1$. Then for $k > 1$, using the above properties, we have

$$\begin{aligned} S^\star(k,j) - jS^\star(k-1,j-1) &= \frac{1}{\sqrt{2\pi}} \int_0^\infty \xi^{k-1} \left[\xi He_j(\xi) - jHe_{j-1}(\xi)\right] \exp(-\xi^2/2)\,\mathrm{d}\xi \\ &= \frac{1}{\sqrt{2\pi}} \int_0^\infty \xi^{k-1} He_{j+1}(\xi) \exp(-\xi^2/2)\,\mathrm{d}\xi \\ &= -\frac{1}{\sqrt{2\pi}} \int_0^\infty \xi^{k-1}\,\mathrm{d}[He_j(\xi)\exp(-\xi^2/2)] \\ &= \frac{1}{\sqrt{2\pi}} \int_0^\infty (k-1)\xi^{k-2} He_j(\xi) \exp(-\xi^2/2)\,\mathrm{d}\xi \\ &= (k-1)S^\star(k-2,j). \end{aligned}$$

□

B Relationship between linearized HME and linearized Boltzmann-BGK

In this part, we investigate the relationship between the linearized Boltzmann-BGK equation (5.11) with its boundary condition (5.12) and the linearized HME for Kramers' problem (4.1) (4.2). First, take the linearized moment coefficients $\bar{u}_1$ and $\bar{f}_{e_1+ke_2}$, $k \in \mathbb{N}_+$ as

$$\begin{aligned} \bar{u}_1(\bar{y}) &= -\bar{\sigma}_{12}\bar{y} + \frac{1}{\sqrt{2\pi}} \int_{\mathbb{R}} Z(\bar{y},\bar{\xi}) \exp\left(-\frac{\bar{\xi}^2}{2}\right) \mathrm{d}\bar{\xi}, \\ \bar{f}_{e_1+ke_2}(\bar{y}) &= \frac{1}{k!}\frac{1}{\sqrt{2\pi}} \int_{\mathbb{R}} He_k(\bar{\xi}) Z(\bar{y},\bar{\xi}) \exp\left(-\frac{\bar{\xi}^2}{2}\right) \mathrm{d}\bar{\xi} \end{aligned} \tag{B.1}$$

by $Z(\bar{y},\bar{\xi})$ in (5.13), and note that the linearized Boltzmann-BGK equation (5.11) is an integral equation on $\bar{\xi}$ and a differential equation on $\bar{y}$. Then we discretize it with respect to $\bar{\xi}$ by the Gauss-Hermite quadrature

with $M \in \mathbb{N}$ points. Denote the weights and integral points of Gauss-Hermite quadrature by ω_i and $\bar{\xi}_i$, $i = 1, \cdots, M$, respectively. If we choose $\bar{\xi}_i$ such that $\bar{\xi}_i > \bar{\xi}_{i-1}$, where $\bar{\xi}_i$, $i = 1, \cdots, M$ are zeros of $He_M(x)$, then $\bar{\xi}_i = \lambda_i$ in (4.8). Let $\boldsymbol{\omega} = (\omega_1, \cdots, \omega_M)^T$ and $\boldsymbol{Z}(\bar{y}) = (Z_1(\bar{y}), \cdots, Z_M(\bar{y}))^T$, where $Z_k(\bar{y}) = Z(\bar{y}, \bar{\xi}_k)$, then the discretization of (5.11) can be written as

$$K_0 \boldsymbol{\Lambda} \mathbf{1} + \boldsymbol{\Lambda} \frac{\mathrm{d}\boldsymbol{Z}(\bar{y})}{\mathrm{d}\bar{y}} = \left(\mathbf{1}\boldsymbol{\omega}^T - \mathbf{I}\right) \boldsymbol{Z}(\bar{y}), \tag{B.2}$$

where $\boldsymbol{\Lambda} = \mathrm{diag}\{\bar{\xi}_i; i = 1, \cdots, M\}$ is the same as the matrix (4.7), $\mathbf{I}$ is the $M \times M$ identity matrix, and $\mathbf{1} = (1, \cdots, 1)^T \in \mathbb{R}^M$. The boundary condition (5.12) can be discretized as

$$Z(0, \bar{\xi}_i) = (1 - \chi) Z(0, -\bar{\xi}_i), \quad i = 1, \ldots, m. \tag{B.3}$$

Next, we aim to show that the linearized HME (4.1) is equivalent to the discrete linearized Boltzmann-BGK equation (B.2) for Kramers' problem. Let $\mathbf{W} = \mathrm{diag}\{\omega_i;\ i = 1, \ldots, M\}$. Since $\mathbf{W}$ is a constant matrix which independent of $\bar{y}$, $\mathbf{W}$ and $\boldsymbol{\Lambda}$ are both diagonal matrices, the upper formulation can be rewritten as

$$K_0 \boldsymbol{\Lambda} \mathbf{W} \mathbf{1} + \boldsymbol{\Lambda} \frac{\mathrm{d}\mathbf{W}\boldsymbol{Z}(\bar{y})}{\mathrm{d}\bar{y}} = \left(\mathbf{W}\mathbf{1}\boldsymbol{\omega}^T \mathbf{W}^{-1} - \mathbf{I}\right) \mathbf{W}\boldsymbol{Z}(\bar{y}). \tag{B.4}$$

Since $\bar{\xi}_i = \lambda_i$, the decomposition of $\mathbf{M}$ in (4.5) indicates $\boldsymbol{\Lambda} = \mathbf{R}^{-1}\mathbf{M}\mathbf{R}$, where $\mathbf{R}$ is defined by (4.6). The orthogonality of the Hermite polynomial indicates $\sum_{i=1}^{M} w_i He_j(\bar{y}_i) = \delta_{j,0}$, thus we have

$$\mathbf{R}\mathbf{W}\mathbf{1} = \boldsymbol{e}_1, \quad \boldsymbol{\omega}^T = \boldsymbol{e}_1^T \mathbf{R}\mathbf{W}.$$

Now (B.4) can be rewritten as

$$\begin{aligned} K_0 \boldsymbol{e}_2 + \mathbf{M} \frac{\mathrm{d}[\mathbf{R}\mathbf{W}\boldsymbol{Z}(\bar{y})]}{\mathrm{d}\bar{y}} &= \mathbf{M} \frac{\mathrm{d}V}{\mathrm{d}\bar{y}} \\ &= \mathbf{R}\left(\mathbf{W}\mathbf{1}\boldsymbol{\omega}^T \mathbf{W}^{-1} - \mathbf{I}\right) \mathbf{W}\boldsymbol{Z}(\bar{y}) \\ &= \left(\mathbf{R}\mathbf{W}\mathbf{1}\boldsymbol{\omega}^T \mathbf{W}^{-1}\mathbf{R}^{-1} - \mathbf{I}\right) [\mathbf{R}\mathbf{W}\boldsymbol{Z}(\bar{y})] \\ &= \left(\boldsymbol{e}_1 \boldsymbol{e}_1^T - \mathbf{I}\right) [\mathbf{R}\mathbf{W}\boldsymbol{Z}(\bar{y})] \\ &= -\mathbf{Q}[\mathbf{R}\mathbf{W}\boldsymbol{Z}(\bar{y})], \end{aligned} \tag{B.5}$$

where $\mathbf{Q}$ is defined by (4.5). Direct discretization of (B.1) yields

$$\begin{aligned} \bar{u}_1(\bar{y}) &= K_0 \bar{y} + \sum_{j=1}^{M} \omega_j Z_j(\bar{y}) = [\mathbf{R}\mathbf{W}\boldsymbol{Z}(\bar{y})]_1 + K_0 \bar{y}, \\ \bar{f}_{e_1 + k e_2}(\bar{y}) &= \frac{1}{k!} \sum_{j=1}^{M} \omega_j He_k(\bar{\xi}_j) Z_j(\bar{y}) = [\mathbf{R}\mathbf{W}\boldsymbol{Z}(\bar{y})]_{k+1}, \quad k = 1, \ldots, M-1, \end{aligned}$$

which indicate

$$V(\bar{y}) = \mathbf{R}\mathbf{W}\boldsymbol{Z}(\bar{y}) + K_0 \bar{y}. \tag{B.6}$$

Substituting (B.6) into (B.5) to eliminate $\mathbf{R}\mathbf{W}\boldsymbol{Z}(\bar{y})$, we obtain

$$\mathbf{M} \frac{\mathrm{d}V(\bar{y})}{\mathrm{d}\bar{y}} = -\mathbf{Q}V(\bar{y}), \tag{B.7}$$

which is the same as (4.3).

Finally, let us check the relationship between (4.2) and the discretized boundary condition (B.3). Since the zeros of Hermite polynomials are symmetric in regard to 0, (B.3) can be written as

$$\omega_i Z(0, \bar{\xi}_i) = (1 - \chi) \omega_{M+1-i} Z(0, \bar{\xi}_{M+1-i}), \quad i = 1, \ldots, m. \tag{B.8}$$

Here we remind that $m = \lfloor \frac{M}{2} \rfloor$. Define the matrix $\mathbf{H}_\chi$ as

$$\mathbf{H}_\chi = \begin{pmatrix} 1 & & & & \chi-1 \\ & \ddots & & \iddots & \\ & & 1 & \chi-1 & \end{pmatrix}_{m\times M}, \qquad \text{if } M \text{ is even},$$

$$\mathbf{H}_\chi = \begin{pmatrix} 1 & & 0 & & \chi-1 \\ & \ddots & \vdots & \iddots & \\ & & 1 \quad 0 & \chi-1 & \end{pmatrix}_{m\times M}, \qquad \text{if } M \text{ is odd},$$

then (B.8) can be reformulated as

$$\mathbf{H}_\chi \mathbf{W} \boldsymbol{Z}(0) = 0. \tag{B.9}$$

Let

$$\mathbf{K} = \frac{1}{\chi} \begin{pmatrix} \bar{\xi}_1 & \bar{\xi}_2 & \cdots & \bar{\xi}_m \\ \bar{\xi}_1^3 & \bar{\xi}_2^3 & \cdots & \bar{\xi}_m^3 \\ \vdots & \vdots & \ddots & \vdots \\ \bar{\xi}_1^{2m-1} & \bar{\xi}_2^{2m-1} & \cdots & \bar{\xi}_m^{2m-1} \end{pmatrix}_{m\times m}.$$

Since $\bar{\xi}_1, \cdots, \bar{\xi}_m$ are distinct, $\mathbf{K}$ is invertible due to the invertibility of Vandermonde matrix. Noticing (B.6), we can simplify (B.9) as

$$\mathbf{K}\mathbf{H}_\chi \mathbf{W} \left(\mathbf{W}^{-1}\mathbf{R}^{-1} V(0)\right) = \mathbf{K}\mathbf{H}_\chi \mathbf{R}^{-1} V(0) = 0. \tag{B.10}$$

What we need to verify is that (B.10) is equivalent to (4.4). Next we just need to prove that $\mathbf{B} = \mathbf{K}\mathbf{H}_\chi\mathbf{R}^{-1}$.

Let $\tilde{\mathbf{R}} = (\tilde{r}_{ij})_{M\times M}$ with $\tilde{r}_{ij} = He_{i-1}(\lambda_j)$, $i, j = 1, \ldots, M$, then from (4.6), one obtains $\mathbf{R} = \text{diag}\left\{1, 1, \frac{1}{2!}, \ldots, \frac{1}{(M-1)!}\right\}\cdot \tilde{\mathbf{R}}$. Using the orthogonality of Hermite polynomials

$$\frac{1}{\sqrt{2\pi}} \int_{\mathbb{R}} He_j(x) He_k(x) \exp\left(-\frac{x^2}{2}\right) \mathrm{d}x = j!\delta_{jk},$$

one obtains

$$\mathbf{W}\tilde{\mathbf{R}}^T\mathbf{R} = \mathbf{I}.$$

The discretization of $S(k, j)$ in (3.7c) is

$$\begin{aligned} S(k,j) &= \frac{1}{\chi} \sum_{n=1}^{m} \left(\bar{\xi}_n^k \omega_n \left(He_j(\bar{\xi}_n) - (1-\chi) He_j(-\bar{\xi}_n)\right)\right) \\ &= \frac{1}{\chi} (\bar{\xi}_1^k, \bar{\xi}_2^k, \ldots, \bar{\xi}_m^k) \cdot \mathbf{H}_\chi \mathbf{W} \cdot \left(He_j(\bar{\xi}_1), He_j(\bar{\xi}_2), \ldots, He_j(\bar{\xi}_M)\right)^T, \end{aligned}$$

then

$$\mathbf{K}\mathbf{H}_\chi \mathbf{W}\tilde{\mathbf{R}}^T = \mathbf{B}.$$

References

[1] P. L. Bhatnagar, E. P. Gross, and M. Krook. A model for collision processes in gases. I. small amplitude processes in charged and neutral one-component systems. Phys. Rev., 94(3):511–525, 1954.

[2] G. A. Bird. Molecular Gas Dynamics and the Direct Simulation of Gas Flows. Oxford: Clarendon Press, 1994.

[3] L. Boltzmann. Weitere studien über das wärmegleichgewicht unter gas-molekülen. Wiener Berichte, 66:275–370, 1872.

[4] Z. Cai, Y. Fan, and R. Li. Globally hyperbolic regularization of Grad's moment system in one dimensional space. Comm. Math. Sci., 11(2):547–571, 2013.

[5] Z. Cai, Y. Fan, and R. Li. Globally hyperbolic regularization of Grad's moment system. Comm. Pure Appl. Math., 67(3):464–518, 2014.

[6] Z. Cai, Y. Fan, and R. Li. On hyperbolicity of 13-moment system. Kinetic and Related Models, 7(3):415–432, 2014.

[7] Z. Cai, Y. Fan, R. Li, and Z. Qiao. Dimension-reduced hyperbolic moment method for the Boltzmann equation with BGK-type collision. Commun. Comput. Phys., 15(5):1368–1406, 2014.

[8] Z. Cai, R. Li, and Z. Qiao. NRxx simulation of microflows with Shakhov model. SIAM J. Sci. Comput., 34(1):A339–A369, 2012.

[9] Z. Cai, R. Li, and Z. Qiao. Globally hyperbolic regularized moment method with applications to microflow simulation. Computers and Fluids, 81:95–109, 2013.

[10] C. Cercignani. Mathematical Methods in Kinetic Theory. Springer US, New York, 1969.

[11] S. Chapman. On the law of distribution of molecular velocities, and on the theory of viscosity and thermal conduction, in a non-uniform simple monatomic gas. Phil. Trans. R. Soc. A, 216(538–548):279–348, 1916.

[12] N. Dongari, R. Sambasivam, and F. Durst. Extended Navier-Stokes equations and treatments of microchannel gas flows. Journal of Fluid Science and Technology, 4(2):454–467, 2009.

[13] Y. Fan and R. Li. Globally hyperbolic moment system by generalized Hermite expansion. arXiv:1401.4639, 2014.

[14] R. D. M. Garcia and C. E. Siewert. The linearized Boltzmann equation with Cercignani-Lampis boundary conditions: Basic flow problems in a plane channel. Eur. J. Mech. B/Fluids, 28(3):387–396, 2009.

[15] H. Grad. On the kinetic theory of rarefied gases. Comm. Pure Appl. Math., 2(4):331–407, 1949.

[16] A. Grucelski and J. Pozorski. Lattice Boltzmann simulations of flow past a circular cylinder and in simple porous media. Computers and Fluids, 71:406 – 416, 2013.

[17] X. J. Gu, D. R. Emerson, and G. H. Tang. Kramers' problem and the Knudsen minimum: a theoretical analysis using a linearized 26-moment approach. Continuum Mech. Thermodyn., 21:345–360, 2009.

[18] X. J. Gu, D. R. Emerson, and G. H. Tang. Analysis of the slip coefficient and defect velocity in the knudsen layer of a rarefied gas using the linearized moment equations. Phys. Rev. E, 81:016313, Jan 2010.

[19] Z. Guo, T. S. Zhao, and Y. Shi. Generalized hydrodynamic model for fluid flows: From nanoscale to macroscale. Physics of Fluids, 18(6), 2006.

[20] F. J. Higuera and S. Succi. Simulating the flow around a circular cylinder with a lattice Boltzmann equation. EPL (Europhysics Letters), 8(6):517, 1989.

[21] G. E. Karniadakis, A. Beskok, and N. Aluru. Microflows: Fundamentals and Simulation. Springer-Verlag New York, 2002.

[22] T. Klinc and I. Kuscer. Slip coefficients for general gas-surface interaction. Phys. Fluids, 15:1018, 1972.

[23] H. A. Kramers. On the behaviour of a gas near a wall. Il Nuovo Cimento (1943-1954), 6(2):297–304, 1949.

[24] S. Lang. Algebra revised third edition. Graduate Texts in Mathematics, 1(211):ALL–ALL, 2002.

[25] C. D. Levermore. Moment closure hierarchies for kinetic theories. J. Stat. Phys., 83(5–6):1021–1065, 1996.

[26] C. R. Lilley and J. E. Sader. Velocity gradient singularity and structure of the velocity profile in the Knudsen layer according to the Boltzmann equation. Phys. Rev. E, 76:026315, Aug 2007.

[27] D. A. Lockerby and J. M. Reese. On the modelling of isothermal gas flows at the microscale. Journal of Fluid Mechanics, 604:235–261, 6 2008.

[28] S. K. Loyalka and J. H. Ferziger. Model dependence of the slip coefficient. Phys. Fluids, 10:1833, 1967.

[29] S. K. Loyalka and K. A. Hickey. The Kramers problem: Velocity slip and defect for a hard sphere gas with arbitrary accommodation. Z. Angew. Math. Phys., 41:245, 1990.

[30] S. K. Loyalka and Z. Naturforsch. Approximate method in kinetic theory. Phys. Fluids, 14:2291–2294, 1971.

[31] S. K. Loyalka, N. Petrellis, and T. S. Storvick. Some numerical results for the BGK model: Thermal creep and viscous slip problems with arbitrary accomodation at the surface. Physics of Fluids, 18(9):1094–1099, 1975.

[32] W. Marques Jr. and G. M. Kremer. Couette flow from a thirteen field theory with slip and jump boundary conditions. Continuum Mechanics and Thermodynamics, 13(3):207–217, 2001.

[33] J. C. Maxwell. On stresses in rarefied gases arising from inequalities of temperature. Proc. R. Soc. Lond., 27(185–189):304–308, 1878.

[34] S. Mizzi, R. W. Barber, D. R. Emerson, J. M. Reese, and S. K. Stefanov. A phenomenological and extended continuum approach for modelling non-equilibrium flows. Continuum Mechanics and Thermodynamics, 19(5):273–283, 2007.

[35] I. Müller and T. Ruggeri. Rational Extended Thermodynamics, Second Edition, volume 37 of Springer tracts in natural philosophy. Springer-Verlag, New York, 1998.

[36] J. M. Reese, M. A. Gallis, and D. A. Lockerby. New directions in fluid dynamics: non-equilibrium aerodynamic and microsystem flows. Philosophical Transactions of the Royal Society of London A: Mathematical, Physical and Engineering Sciences, 361(1813):2967–2988, 2003.

[37] C. E. Siewert. Kramers' problem for a variable collision frequency model. European Journal of Applied Mathematics, 12:179–191, 4 2001.

[38] H. Struchtrup. Kinetic schemes and boundary conditions for moment equations. Z. Angew. Math. Phys., 51(3):346–365, 2000.

[39] H. Struchtrup. Grad's moment equations for microscale flows. In A. D. Ketsdever and E. P. Muntz, editors, Rarefied Gas Dynamics: 23rd International Symposium, volume 663, pages 792–799. AIP, 2003.

[40] M. Torrilhon. Special issues on moment methods in kinetic gas theory. Continuum Mech. Thermodyn., 21(5):341–343, 2009.

[41] M. Torrilhon and H. Struchtrup. Boundary conditions for regularized 13-moment-equations for micro-channel-flows. J. Comput. Phys., 227(3):1982–2011, 2008.

[42] M. M. R. Williams. A review of the rarefied gas dynamics theory associated with some classical problems in flow and heat transfer. Zeitschrift für angewandte Mathematik und Physik ZAMP, 52(3):500–516, 2001.

[43] W.M. Zhang, G. Meng, and X.Y. Wei. A review on slip models for gas microflows. Microfluidics and Nanofluidics, 13(6):845–882, 2012.